# PHARMACOLOGICAL AND GENETIC RESCUE OF IDIOPATHIC EPILEPSIES

By

Lyndsey Leigh Anderson

Dissertation

Submitted to the Faculty of the

Graduate School of Vanderbilt University

in partial fulfillment of the requirements

for the degree of

DOCTOR OF PHILOSOPHY

in

Pharmacology

May, 2014

Nashville, Tennessee

Approved:

Afred George Jr., M.D.

Vsevolod Gurevich, Ph.D.

Jennifer Kearney, Ph.D.

Robert Macdonald, M.D., Ph.D.

Gregg Stanwood, Ph.D.

To those whose lives are

affected by epilepsy

ACKNOWLEDGEMENTS

First and foremost, I must acknowledge my mentor, Dr. Alfred George Jr. I could not have asked for a better mentor for my graduate school experience, as I know that I have grown leaps and bounds as a scientist from the training I received from Dr. George. He has always challenged me to think critically and independently. I really appreciate the skills that I have developed as a scientific thinker, writer and researcher under the guidance of Dr. George. I am forever grateful for my time spent in Dr. George's lab, and I look forward to beginning the next chapter of my career with him at Northwestern.

Additionally, I have to say a huge 'thank you' to all the members of the George lab, both past and present. I am lucky to call you guys friends. You are all amazing people and our unique lab dynamic has made it enjoyable to come into lab every morning. We all worked hard but had a lot of fun along the way, a large part due to our lab manager, Jennifer Kunic. She has taken care of so many things that I know are often times taken for granted. I am grateful for her kind, caring heart and all that she has done for me and the George lab as a whole. I would also like to acknowledge Chris Thompson for all that he has taught me over my graduate school experience. Not only did Chris directly contribute a great deal to my thesis project, but I have learned so much from him about the ins and outs of ion channels, scientific writing, experimental design and life in general.

I must also acknowledge our neighbors in the Kearney lab. In many regards, Dr. Kearney has been my co-mentor and I have felt like an adopted member of her lab. She has extensive expertise in epilepsy and with mouse colonies, and I have very much appreciated all that she has taught me and the mentorship that she has provided over the years. I am appreciative for all of Clint McCollom's help with my mouse husbandry and the genotyping that he performed. Additionally, I must acknowledge my colleague and friend Nicole Hawkins. Whether we were performing mouse surgeries or learning mass spectrometry, there was always a lot of laughter and fun. Thanks for all of the memories.

I am grateful for each of the additional members of my thesis committee, Seva Gurevich, Bob Macdonald and Gregg Stanwood, whose suggestions and enthusiasm during my committee meetings all contributed to the success of my project.

Lastly, I would like to express my appreciation for all the support that I received from my friends and family during my time in Nashville. Throughout the course of my graduate school experience, I was fortunate enough to meet many wonderful and intelligent people here. I enjoyed all of scientific discussions over beers in addition to all of our wild adventures. You have all made Nashville a special place, and I look forward to watching the paths that your lives take in the future. Words cannot express the magnitude of appreciation that I have for the love and support of my family. Although most times they have no idea why I love science or what I am talking about, their feigned excitement is much appreciated. Thank you for all that you have done for me!

TABLE OF CONTENTS

LIST OF TABLES

LIST OF FIGURES

Figure Page

LIST OF ABBREVIATIONS

**General Abbreviations**

| | |
|---|---|
| AED | antiepileptic drug |
| MES | maximal electroshock |
| PTZ | pentylenetetrazole |
| $Na_v$ | voltage-gated sodium channel |
| α-subunit | the major pore forming subunit of the voltage-gated sodium channel |
| β-subunit | the auxiliary subunit of the voltage-gated sodium channel |
| *SCN1A* | human voltage-gated sodium channel α-subunit isoform 1 gene |
| *SCN1B* | human voltage-gated sodium channel β-subunit isoform 1 gene |
| GABA | gamma-aminobutyric acid |
| *Scn2a*$^{Q54}$ | transgenic mouse expressing mutant $Na_v1.2$ (GAL879-881QQQ) |
| B6.Q54 | *Scn2a*$^{Q54}$ mouse congenic on background strain C57BL/6J |
| F1.Q54 | *Scn2a*$^{Q54}$ mouse generated by a cross between a B6.Q54 hemizygous mouse and an SJL/J mouse |
| *Scn1a* | mouse voltage-gated sodium channel α-subunit isoform 1 gene |
| *Scn1a*$^{+/-}$ | mouse with heterozygous knockout of *Scn1a* |
| *Scn1a*$^{RX/+}$ | knock-in mouse line carrying a premature stop codon, R1407X, in *Scn1a* |
| 129.*Scn1a*$^{+/-}$ | *Scn1a*$^{+/-}$ mouse congenic on background strain 129S6/SvEvTac |
| F1.*Scn1a*$^{+/-}$ | *Scn1a*$^{+/-}$ mouse generated by a cross between a 129. *Scn1a*$^{+/-}$ mouse and a C57BL/6J mouse |

| | |
|---|---|
| *Gad67-SCN1A* | *Gad67* promoter driving expression of *SCN1A* selectively in GABAergic interneurons |
| *SCN1A*$^{Tg/+}$ | *Gad67-SCN1A* heterozygous mice |
| GS967 | compound GS-458967 developed by Gilead Sciences |
| B6.*SCN1A*$^{Tg/+}$ | *Gad67-SCN1A* heterozygous mice maintained on background strain C57BL/6J |
| *Scn1a*$^{+/-}$ :: *SCN1A*$^{Tg/+}$ | combined knockout/transgenic mice that have one wildtype allele, the knockout allele and one copy of the *Gad67-SCN1A* transgene |
| WT | wildtype |

# CHAPTER I

# INTRODUCTION

## *Epilepsy*

Epilepsy is a common neurological disorder affecting 1% of the population worldwide, and is characterized by recurrent, unprovoked seizures resulting from synchronous neuronal discharges.[1-4] An imbalance between excitatory and inhibitory neurotransmission is the neurophysiological hallmark of epilepsy. The term epilepsy encompasses a heterogeneous group of disorders that vary in severity, etiology and seizure type. The classification and diagnosis of epilepsies is based on two features: the seizure type and the underlying cause. In order to generate a consistent vocabulary that reflects the current state of our knowledge and understanding of epilepsies, in 2010 the International League Against Epilepsy revised the terminology for classifying seizures and etiology of epilepsy.

Clinically, seizures can be classified into two categories: focal or generalized. Focal seizures originate in a localized brain region that constitutes the seizure focus that is consistent from one seizure to another. Features of focal seizures such as the impairment of consciousness or awareness, progression of seizure events and dyscognitive characteristics are descriptors used by clinicians for evaluating patients. Generalized seizures, on the other hand, involve both hemispheres from the outset, rapidly engaging

bilaterally distributed networks and can be separated into several subcategories: tonic-clonic, absence, myoclonic or others (less common).[4-6] Tonic-clonic seizures are divided into two phases, the tonic phase where flexor and extensor muscles are simultaneously activated throughout the body resulting in a stiffening, followed by the clonic phase with a repetitive, rhythmic convulsion of muscles. Absence seizures are characterized by a brief episode of unresponsiveness with loss of consciousness. Myoclonic seizures are very brief muscle contractions involving the whole body or part of the body.

The three terms genetic, structural/metabolic and unknown have been adopted for the etiological classification of epilepsies. Genetic epilepsies are the direct result of a known or presumed genetic defect in which seizures are the core symptom of the disorder. In order to presume a genetic basis, either a gene and the molecular mechanisms should be identified or an appropriately designed family study should provide evidence of a genetic component. Structural/metabolic epilepsies are a secondary result of a distinct other structural or metabolic condition. Structural lesions associated with an increased risk of epilepsy may be acquired or of genetic origin. However, these are distinct from "genetic epilepsies" because there is believed to be a separate disorder between the genetic defect and the epilepsy. Lastly, the classification of unknown is used to reflect epilepsies in which the underlying cause is unknown and makes no assumptions regarding cause.[6] Albeit somewhat simple, these classifications have enabled clinicians to diagnose the epilepsy type and select the most effective treatment strategy for each patient.

*Treatments of epilepsy*

The only existing cure for epilepsy is resective surgery for suitable patients and thus treatment of the majority of epilepsy patients with the currently available antiepileptic drugs (AEDs) is only symptomatic. There are approximately twenty-four FDA approved antiepileptic drugs on the market with various mechanisms of action but most function to dampen neuronal signaling either by enhancing GABA-mediated inhibition or controlling excitability through actions on $Na^{+}$ channels or T-type $Ca^{+2}$ channels.[7] Although many epilepsy patients achieve complete seizure control with current AEDs, these medications fail to control seizures in 30% of patients, highlighting the need not only for novel AEDs but also for research into the underlying molecular mechanisms of epilepsy that will contribute to our understanding of this debilitating disease.[3]

*Antiepileptic drug discovery*

Animal models of epilepsy have aided in our effort to understand the pathogenesis of epilepsy and have been instrumental for AED discovery. The development of AEDs predominantly relies on the screening of test compounds for predictive activity against specific seizure types mimicked by acute seizure models, namely the maximal electroshock (MES) and pentylenetetrazole (PTZ) models.[8] The MES seizure test was introduced in cats in 1937 and adapted for rodents in 1946.[9,10] In the MES seizure model an electrical stimulus is administered either transcorneally or transauricularily to induce generalized tonic-clonic seizures.[10] PTZ, a chemical convulsant, induces myoclonic and clonic convulsions. Additional induced epilepsy models include kindling, kainate and

pilocarpine. Amygdala kindling describes a process in which an electrical stimulus is administered to the amygdala via depth electrodes. Repeated administration of the initially subconvulsive stimuli eventually induces seizures that increase in severity and duration.[11] Kindling models are used to identify compounds that are predicted to be active against focal seizures in patients. Both kainate and pilocarpine models of epilepsy exhibit spontaneous, recurrent seizures following the initial induction of *status epilepticus* with administration of either agent.[12-14] The only genetic model of epilepsy being used for late-stage screening of AEDs is the GAERs rat which exhibits absence seizures.[15] The 6-Hz psychomotor seizure model in which a prolonged electrical stimulus induces seizures has more recently been employed as a drug-resistant model in AED screens.[16] All the models described, with the exception of the GAERs rat, represent induced seizure models occurring in non-epileptic brains and therefore do not accurately reflect the epilepsy process. Since the introduction of these models and the establishment of the Anticonvulsant Screening Project of NIH/NINDS, numerous effective antiepileptic drugs have been generated. However, this screening process, relatively unchanged since 1978 and reliant upon non-physiological models of epilepsy, has led to the stagnation of the development of new AEDs. This is a significant problem as 30% of epilepsy patients remain without effective treatment options.[3,8] The new generation of genetic epilepsy models which recapitulate spontaneous epilepsy in humans has been proposed as alternatives for the AED development and screening process.[8]

*Etiology of epilepsy*

In addition to having utility in drug discovery, genetic models of epilepsy are being used to advance our knowledge regarding the pathology of epilepsy. While disease and injury to the central nervous system are known to contribute to seizure susceptibility, the cellular and molecular mechanisms that underlie the pathogenesis of most epilepsies remain largely unknown (Figure 1.1).[1] Previous work, however, has suggested the importance of genetic factors to the development of epilepsy.[17] Although genetic epilepsies exhibit complex inheritance patterns, genetic mapping has identified mutations in single genes that are responsible for epilepsy in human patients. All of the mutations that have been identified are molecular components of neuronal signaling, with mutations in voltage-gated sodium channels being the most prevalent.[17]

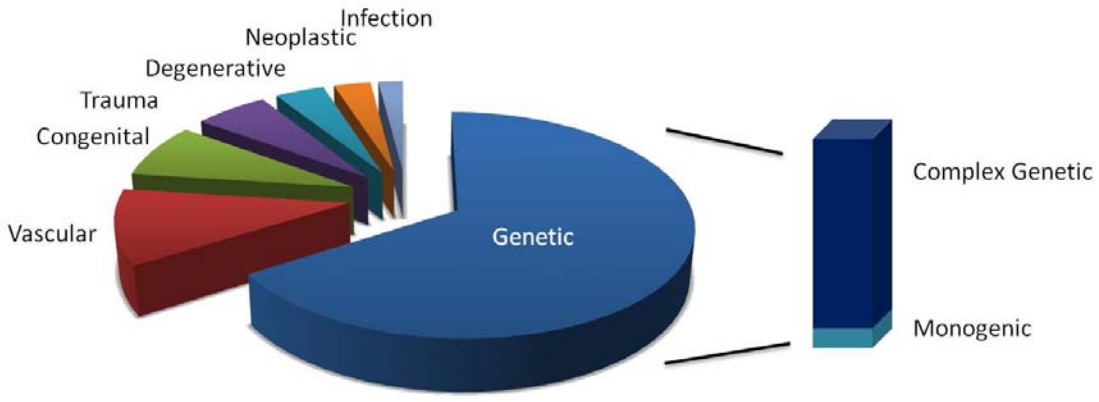


**Figure 1.1.** Proportion of cases of epilepsy by etiology (Adapted from Hauser *et al*, 1993).

*Voltage-gated sodium channels*

Voltage-gated sodium channels are responsible for the initiation and propagation of action potentials in electrically excitable cells such as nerve, skeletal muscle and heart.

Voltage-gated sodium ($Na_v$) channels are integral membrane proteins consisting of a pore-forming α-subunit (260 kD) complexed with one or more auxiliary β-subunits (33-40 kD) (Figure 1.2).[18-21] Nine genes encoding distinct α-subunits and four encoding β-subunits have been identified in the human genome and the isoforms exhibit variable tissue expression patterns (Table 1.1).[21] The α-subunit is composed of four structurally homologous domains (D1-D4) each containing six transmembrane segments (S1-S6). When the α-subunit adopts its three-dimensional structure within the membrane, it creates an ion-conducting pore with ion selectivity and permeation controlled by the S5-S6 pore loop of each domain. The S4 segment of each domain contains basic amino acids (arginine or lysine) at every third position and functions as a voltage-sensor.[18-20] The β-subunits are single transmembrane proteins that modify the kinetics and voltage-dependence of gating of the α-subunit. Accessory β-subunits are also involved in channel localization and interact with other signaling molecules and the cytoskeleton making them an essential component of the $Na_v$ channel macromolecular complex.[21,22]

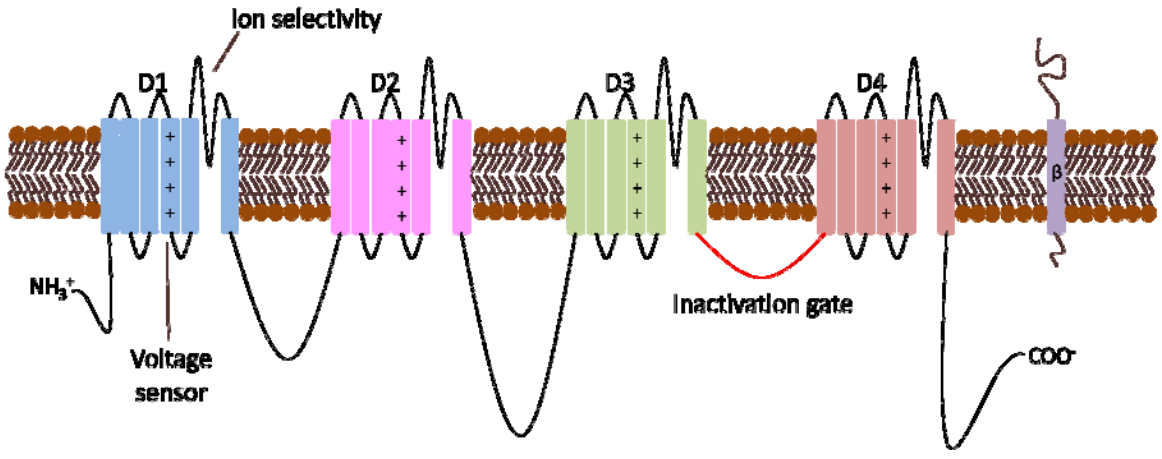


**Figure 1.2.** Schematic representation of a single voltage-gated sodium channel α-subunit and auxiliary β-subunit.

Given the importance of $Na_v$ channels to action potential generation and neuronal signaling, it is not surprising that more than 800 mutations in $Na_v$ channels have been identified in association with a range of clinically diverse epilepsies.[20,21,23] Mutations within $Na_v1.1$ constitute the greatest number of mutations identified; however, mutations within $Na_v1.2$, $Na_v1.3$, $Na_v1.6$ and the $\beta_1$ subunit have also been described.[17,24] Utilizing whole-cell electrophysiology, researchers have been able to characterize the biophysical properties of these disease-associated mutant channels. High resolution functional characterization of several mutations has provided insight on the molecular mechanisms by which voltage-gated sodium channel dysfunction contributes to epileptogenesis. Interestingly, the mutations identified exhibit altered biophysical properties representative of both gain-of-function and loss-of-function phenotypes.

**Table 1.1.**
Mammalian voltage-gated sodium channel genes

| Gene | Protein | Tissue Expression |
|---|---|---|
| *SCN1A* | $Na_v1.1$ | CNS, PNS, cardiac muscle* |
| *SCN2A* | $Na_v1.2$ | CNS, PNS |
| *SCN3A* | $Na_v1.3$ | CNS, PNS |
| *SCN4A* | $Na_v1.4$ | skeletal muscle |
| *SCN5A* | $Na_v1.5$ | cardiac muscle, skeletal muscle* |
| *SCN8A* | $Na_v1.6$ | CNS, PNS, cardiac muscle* |
| *SCN9A* | $Na_v1.7$ | PNS |
| *SCN10A* | $Na_v1.8$ | PNS |
| *SCN11A* | $Na_v1.9$ | PNS |

CNS, central nervous system; PNS, peripheral nervous system; *minor expression (Adapted from Meisler and Kearney, 2005).

Gain-of-function mutations within $Na_v$ channels are believed to enhance neuronal excitability thereby increasing seizure susceptibility. Functional studies of epilepsy-associated mutations have shown biophysical abnormalities in both activation and inactivation parameters that are predicted to promote excitability. The *SCN1A* mutation W1204R exhibits a hyperpolarized shift in the voltage-dependence of activation which is consistent with hyperexcitability.[25-27] A depolarized shift in the voltage-dependence of inactivation as observed with the mutations T875M and D1866Y of *SCN1A* represents gain-of-function in channel activity.[26,28,29] An increased rate in the recovery from inactivation would result in a greater number of channels available to reactivate in response to depolarization. This biophysical defect is observed with the *SCN1A* mutation D188V.[30] A common gain-of-function biophysical defect is impaired channel inactivation leading to increased persistent sodium current.[26,31] For example, the *SCN1A* epilepsy-associated mutation R1648H exhibits a level of persistent sodium current that is ~4.5% of peak current compared to less than 1% for the wildtype channel.[31] Persistent sodium current is hypothesized to reduce the threshold for action potential firing, directly resulting in neuronal hyperexcitability.

Because epilepsy is a disorder that reflects neuronal hyperexcitability, the relationship between epilepsy and gain-of-function mutations in $Na_v$ channels consistent with cellular excitability seems rather intuitive. Functional studies, however, have revealed loss-of-function properties in disease-associated mutants. The first sodium channel mutation identified in association with epilepsy was C121W in the $\beta_1$ subunit gene *SCN1B* which resulted in impaired modulation of the associated subunit.[32] Depolarizing shifts in the

voltage-dependence of activation and reduced sodium current density have been observed in functional studies and are consistent with loss-of-function.[31,33,34] Other mutations have been described as nonfunctional resulting from a failure to conduct sodium ions or defects in protein trafficking reducing cell surface expression.[35,36] In Dravet syndrome, a rare epileptic encephalopathy, more than half of the identified mutations in *SCN1A* introduce frameshifts or premature stop codons suggesting that haploinsufficiency of *SCN1A* is pathogenic.[24,37,38] While initially it may seem counter-intuitive that haploinsufficiency of *SCN1A* would cause epilepsy, its regional expression pattern may shed light on the mechanism by which loss-of-function leads to hyperexcitability rather than hypoexcitability. Studies have shown that distribution of *SCN1A* across brain regions is heterogeneous. Within the hippocampus, *SCN1A* expression is largely dependent upon cell type. Pyramidal neurons express negligible levels of *SCN1A*, whereas, interneurons express significantly higher *SCN1A* levels.[39] The preferential expression of *SCN1A* within interneuron populations suggests that interneuron activity would be affected by loss-of-function of *SCN1A* to a greater extent than would pyramidal neurons. Impaired function of GABAergic interneurons resulting from loss of *SCN1A* function would upset the balance between inhibitory and excitatory neurotransmission, tipping the scale toward network hyperexcitability.

Functional characterization of mutant alleles has allowed researchers to correlate genotype-phenotype relationships with the molecular mechanisms that underlie genetic epilepsies. Along with the functional characterization of epilepsy-associated mutations has come the generation of mouse models harboring patient mutations. Genetic mouse

models of epilepsy have been excellent tools for testing specific disease mechanisms thereby furthering our understanding of the pathophysiology of epilepsy and for evaluating targeted therapeutics. Information gained from both the functional characterization of mutants and the use of mouse models has been instrumental for directing the design of desperately needed novel therapies, with the ultimate goal of developing individualized treatments tailored to each patient mutation. Two mouse models of epilepsy are described in greater detail below.

*Scn2a*$^{Q54}$ *mouse model of epilepsy*

A genetically engineered mouse line, *Scn2a*$^{Q54}$ (Tg(Eno2-Scn2a1*)Q54Mm), expresses a transgene encoding an inactivation impaired neuronal $Na_v1.2$ channel. The mutation, consisting of a substitution of glutamine for three adjacent residues, is located in an evolutionarily conserved region in the linker between transmembrane segments 4 and 5 in domain 2 (GAL879-881QQQ) (Figure 1.3A). In heterologous expression systems, this mutation results in abnormal inactivation with increased persistent sodium current when compared to wildtype channels (Figure 1.3 B-C). Mice expressing the *Scn2a*$^{Q54}$ transgene driven by the neuron-specific enolase promoter exhibit a severe epilepsy phenotype that is characterized by frequent partial seizures corresponding to EEG evidence of a seizure focus in the hippocampus. These short duration partial seizures begin in early life then progress to secondarily generalized seizures, status epilepticus and premature death. Epilepsy in *Scn2a*$^{Q54}$ mice is correlated with persistent sodium current in hippocampal pyramidal neurons. These animals also show histopathological changes such as CA1-CA3 and hilar cell loss, gliosis and mossy fiber sprouting in the

hippocampus which also occur in human epilepsy patients. Transgenic overexpression of wildtype $Na_v1.2$ does not lead to a seizure disorder or reduced lifespan. [40]

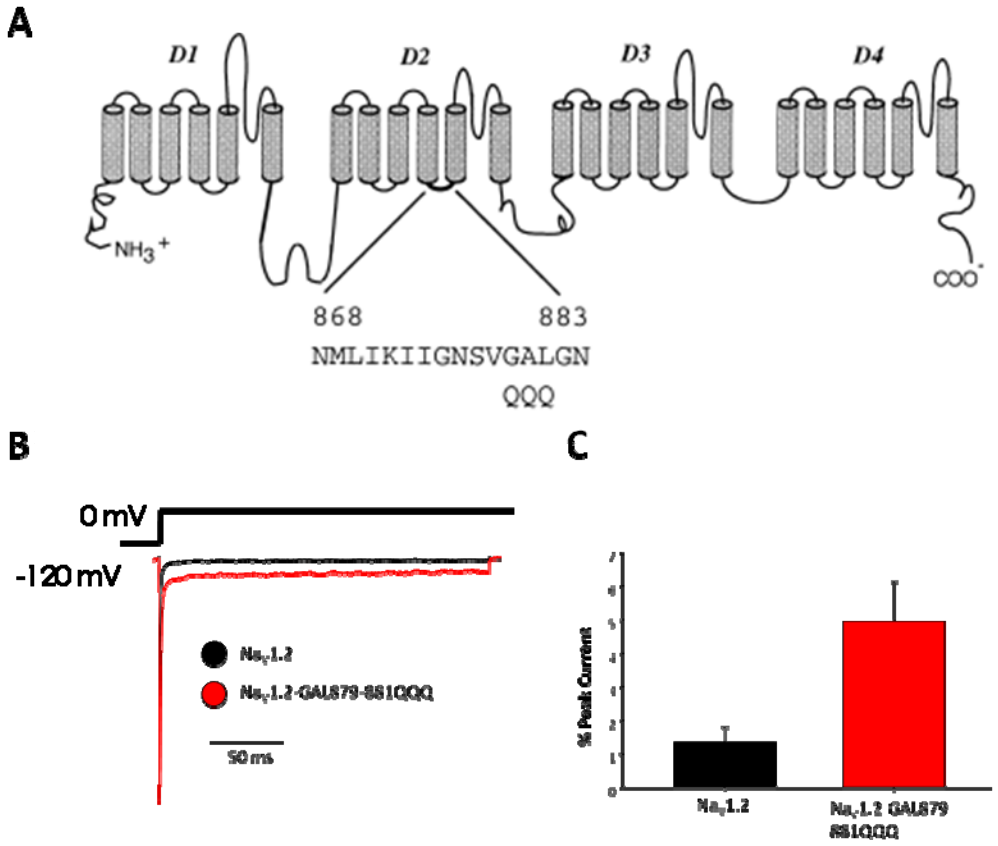


**Figure 1.3.** $Scn2a^{Q54}$ mouse model of epilepsy. (**A**) $Na_V1.2$ mutation (Kearney *et al*, 2001). (**B**) Representative trace of sodium current from wildtype $Na_v1.2$ (black trace) or $Na_v1.2$ GAL879-881QQQ (red trace). (**C**) Summary data for persistent sodium current expressed as % peak current recorded from tsA201 cells - Chris Thompson, PhD.

The severity of the seizure phenotype observed in *Scn2a*$^{Q54}$ mice is influenced by the genetic background. *Scn2a*$^{Q54}$ mice congenic on strain C57BL/6J (B6.Q54) have a seizure onset around 2 months of age with only a 20% incidence at 6 months of age. A cross between hemizygous B6.Q54 males with SJL/J females yields transgenic

heterozygotes on an F1 background (F1.Q54). Seizure onset is around 3 weeks of age in F1.Q54 mice with 100% incidence at 6 months. F1.Q54 mice exhibit a higher seizure incidence, increased seizure severity and reduced lifespan when compared to B6.Q54 mice.[41] Within the F1.Q54 population, female mice exhibit a significantly greater frequency of seizures than males (Figure 1.4). The *Scn2a*$^{Q54}$ mouse, which models mesial temporal lobe epilepsy, provides an excellent model to investigate therapies that would prove effective in patients carrying gain-of-function mutations with persistent sodium current.

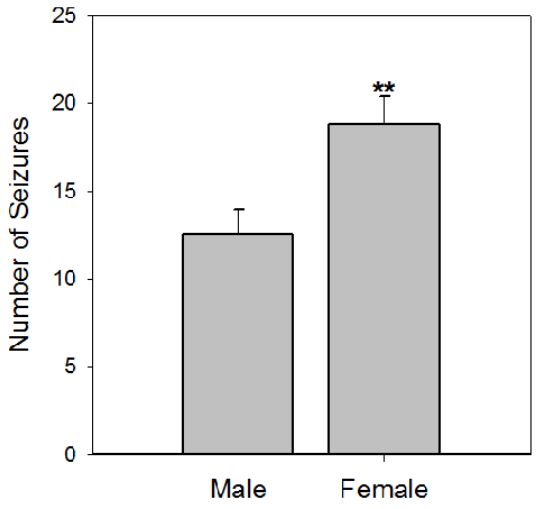


**Figure 1.4.** Scn2a$^{Q54}$ mice exhibit sex differences in seizure frequency. Female F1.Q54 mice exhibit a greater number of seizures than male mice during a 30 minute observation period (** $p < 0.005$).

*Scn1a*$^{+/-}$ *mouse model of epilepsy*

Loss-of-function *SCN1A* mutations have been modeled by *Scn1a* knockout mice, which exhibit a severe epilepsy phenotype mimicking Dravet syndrome. Two groups have generated heterozygous *Scn1a* knockout (*Scn1a*$^{+/-}$) mice and described consistent

phenotypes.[42-44] The first *Scn1a*$^{+/-}$ mouse that was generated by targeted deletion of exon 26 of *Scn1a* (Scn1a$^{tm1Wac}$) was described by the Catterall group in 2006. *Scn1a*$^{+/-}$ mice are reported to exhibit severe, spontaneous generalized tonic-clonic seizures beginning around 2-3 weeks of age, have a reduced seizure threshold and reduced lifespan. Electophysiological recordings of hippocampal interneurons isolated from *Scn1a*$^{+/-}$ mice show a reduction in sodium current density, with no changes in the voltage-dependence of activation or inactivation. Shortly after the introduction of the Catterall *Scn1a*$^{+/-}$ mouse, a knock-in mouse line carrying a premature stop codon, R1407X, in *Scn1a* (Scn1a$^{tm1Kzy}$) was generated and characterized by the Yamakawa group.[39] The *Scn1a*$^{RX/+}$ mouse also models Dravet syndrome with recurrent, spontaneous seizures and premature death. The epilepsy phenotype of Dravet syndrome mice is strongly dependent on genetic background. The Kearney group generated *Scn1a*$^{+/-}$ mice on the 129S6/SvEvTac background (129.*Scn1a*$^{+/-}$) by replacing exon 1 with a neomycin selection cassette (Scn1a$^{tm1Kea}$) and confirmed reduced $Na_v1.1$ expression to ~50% of wildtype levels in brain (Figure 1.5). Heterozygous 129.*Scn1a*$^{+/-}$ mice do not exhibit overt seizures and sporadic death is rare (<10% at 12 weeks). However, when heterozygous 129.*Scn1a*$^{+/-}$ mice are crossed to the C57BL/6J background, F1.*Scn1a*$^{+/-}$ mice are generated. On the mixed genetic background, F1.*Scn1a*$^{+/-}$ mice have frequent seizures with a high incidence of spontaneous death with only 30% survival to 12 weeks (Figure 1.5 C). Results garnered from Dravet syndrome mice have led to the prevailing sentiment that impaired GABA-mediated inhibition is primarily responsible for seizure generation and epileptogenesis in patients exhibiting loss-of-function *SCN1A* mutations.

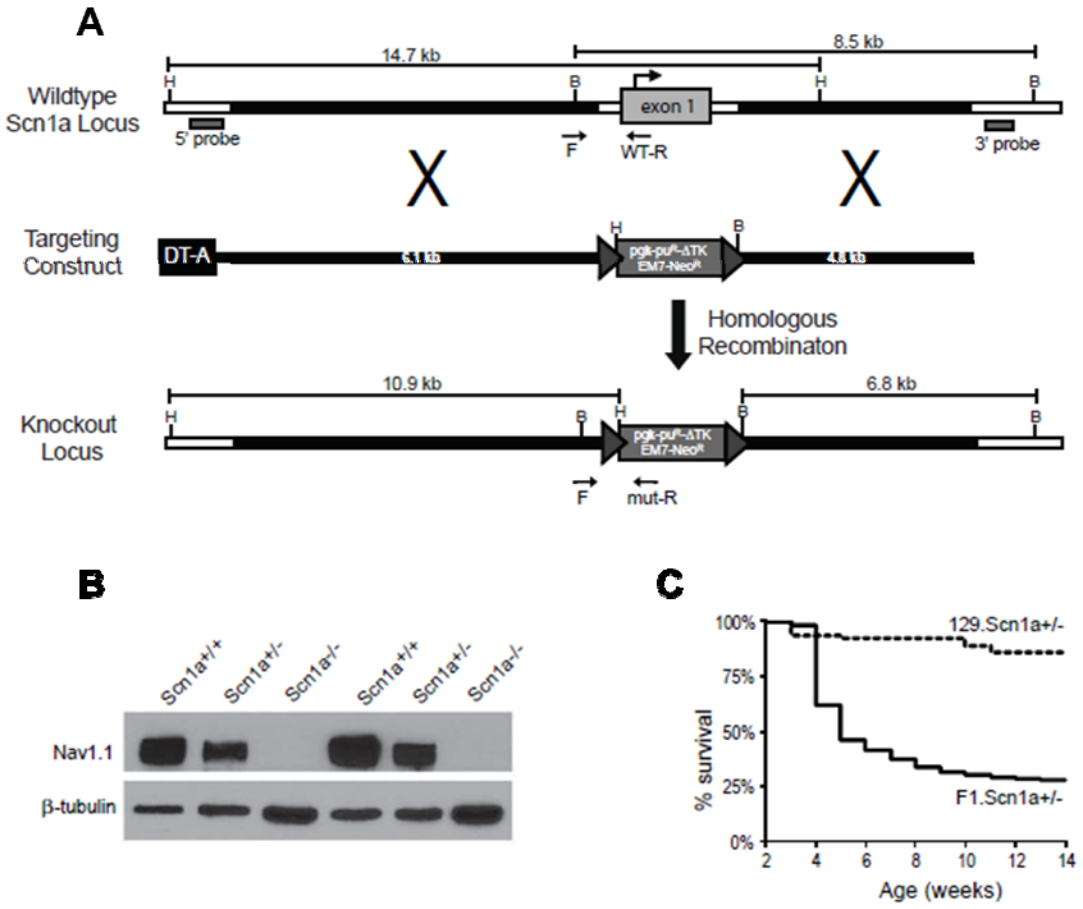


**Figure 1.5.** *Scn1a*$^{+/-}$ mouse model of epilepsy. (**A**) Exon 1 containing the translation start site was replaced by a selection cassette by homologous recombination in ES cells. The targeting vector contained the pGK-puR-Δtk-EM7-NeoR selection cassette flanked by lox sites (triangles), a 6.1 kb 5' homology arm and a 4.8 kb 3' homology arm. The diphtheria toxin cDNA (DT-A) cassette was located outside of the targeting arm for negative selection against random integrations. (**B**) Western blot of brain membrane proteins with a $Na_v1.1$ and β-tubulin antibody. (**C**) Survival of F1.*Scn1a*$^{+/-}$ mice is significantly reduced compared to 129.*Scn1a*$^{+/-}$ mice (Miller *et al*, 2014).

**Specific Aim 1: To determine whether transgenic expression of $Na_v1.1$ in GABAergic neurons would rescue the epilepsy phenotype of *Scn1a*$^{+/-}$ mice.**

We hypothesized that restoration of *SCN1A* selectively in GABAergic interneurons would attenuate or prevent the epilepsy phenotype in *Scn1a*$^{+/-}$ mice. To test this hypothesis, we generated transgenic mice in which human *SCN1A* is expressed selectively in GABAergic neurons using a *Gad67*-specific promoter (*Gad67-SCN1A*). We crossed *Scn1a*$^{+/-}$ mice with *Gad67-SCN1A* transgenic mice to generate a subset of offspring that have one wildtype allele, the knockout allele and one copy of the *Gad67-SCN1A* transgene expressed selectively in inhibitory neurons. We monitored long term survival of combined knockout/transgenic animals (*Scn1a*$^{+/-}$ :: *SCN1A*$^{Tg/+}$) to evaluate whether the mortality associated with *Scn1a*$^{+/-}$ mice could be ameliorated by restoring sodium channel expression in interneurons. Results from these studies provided insight into the potential success of using a genetic approach for the treatment of Dravet syndrome, or inform the development of pharmacological agents that achieve the same degree of restored sodium current.

**Specific Aim 2: To determine whether preferential inhibition of persistent sodium current would be antiepileptic in *Scn2a*$^{Q54}$ mice.**

Increased persistent sodium current has been implicated as a contributor to the pathogenesis of epilepsy. We hypothesized that a drug capable of preferentially suppressing persistent sodium current would be an effective antiepileptic drug. Ranolazine, an FDA-approved drug for the treatment of angina pectoris, and the recently described novel compound, GS-458967 (GS967), selectively inhibit persistent sodium

current. We examined the antiepileptic potential of ranolazine and GS967 in the genetically engineered *Scn2a*$^{Q54}$ mouse model of epilepsy. We tested whether acute treatment with ranolazine or GS967 would reduce seizure frequency of *Scn2a*$^{Q54}$ mice. We also evaluated whether persistent sodium current inhibitors improved survival of *Scn2a*$^{Q54}$ mice. Results from these experiments indicated that preferential inhibition of persistent sodium current represents a novel targeted antiepileptic drug strategy for treating genetic epilepsies associated with gain-of-function voltage-gated sodium channel mutations.

CHAPTER II

# GENERATION OF A TRANSGENIC MOUSE LINE SELECTIVELY EXPRESSING *SCN1A* IN GABAERGIC NEURONS FOR RESCUING DRAVET SYNDROME

## INTRODUCTION

Dravet syndrome, also known as severe myoclonic epilepsy of infancy (SMEI), is a catastrophic pediatric epileptic encephalopathy. Children with Dravet syndrome generally exhibit normal development during the first year of life but then develop seizures often in association with fever, with eventual progression to spontaneous, recurrent seizures and *status epilepticus.* Following the onset of seizures, Dravet syndrome patients develop severe comorbidities including cognitive impairment, ataxia and psychomotor dysfunction.[45,46] Because these children respond poorly to available antiepileptic drugs, there is unfavorable long-term survival.[46,47] More than 70% of Dravet syndrome patients have *de novo* heterozygous mutations in the *SCN1A* gene encoding the voltage-gated sodium channel $\alpha_1$ subunit ($Na_v1.1$).[48,49] Heterozygous missense and truncation mutations suggest haploinsufficiency of *SCN1A* as the genetic mechanism of Dravet syndrome.

Recent studies have demonstrated that heterozygous *Scn1a* knockout ($Scn1a^{+/-}$) mice recapitulate the phenotype of Dravet syndrome. $Scn1a^{+/-}$ mice display spontaneous seizures and premature lethality. They also exhibit a reduced threshold for both hyperthermia- and flurothyl-induced seizures as well as cognitive and motor

impairments.[42-44] Electrophysiological studies in dissociated hippocampal neurons from *Scn1a*$^{+/-}$ mice have shown a reduced sodium current density and impaired excitability in GABAergic interneurons suggesting that impaired GABA-mediated inhibition underlies the pathophysiology of Dravet syndrome.[42,44] To further support this interneuron hypothesis, Cheah *et. al.* generated a conditional deletion mouse model in which $Na_v1.1$ was selectively deleted from forebrain GABAergic interneurons using a Cre-Lox system. Deletion of *Scn1a* selectively from GABAergic interneurons is sufficient to cause epilepsy as the seizure and premature death phenotypes observed in Dravet syndrome are mimicked in this conditional deletion model.[50]

In this study, we generated a transgenic mouse line in which human *SCN1A* is expressed selectively in GABAergic neurons (*Gad67-SCN1A*). We have used this *Gad67-SCN1A* mouse line to directly test the hypothesis that the epilepsy phenotype in Dravet syndrome mice (*Scn1a*$^{+/-}$) can be rescued by restoring sodium channel expression in GABAergic neurons.

## METHODS

### *Animals*

All animal care and experimental procedures were approved by the Vanderbilt University Institutional Animal Care and Use Committee. Mice were group-housed in a pathogen free mouse facility under standard laboratory conditions (12-hr light/dark cycle) and had access to food and water *ad libitum.* *Scn1a*$^{+/-}$ mice were generated as previously described and are maintained as a congenic line on the 129S6/SvEvTac background

(129.*Scn1a*$^{+/-}$).[43] Each *Gad67-SCN1A* transgenic founder was crossed to strain C57BL/6J for at least seven generations to generate an independent line incipient congenic on the C57BL/6J background (B6.*SCN1A*$^{Tg/+}$). Mice used for experiments were from the eighth (N8) or greater backcross generation. Generation of F1 combined knockout/transgenic mice (*Scn1a*$^{+/-}$ :: *SCN1A*$^{Tg/+}$) was carried out by crossing 129.*Scn1a*$^{+/-}$ mice with B6.*SCN1A*$^{Tg/+}$ hemizygous mice. Mice were tail biopsied in the second postnatal week, and DNA was prepared from tail tissue using the Gentra Puregene Mouse tail kit according to the manufacturer's instructions (Qiagen, Valencia, CA). Genotyping of *Scn1a*$^{+/-}$ mice was performed as previously described.[43] Genotyping of the *Gad67-SCN1A* transgene was performed by multiplex PCR with primers A (5' CTC CTC TTC TGC CCG TTC AC 3'), B (5' ATA AGC ACG GGT AGT GAAG 3') and C (5' GAA GAT GGC CTT CCC TTT ATTC 3'). Amplification was initiated by denaturation for 2 minutes at 94$^{o}$C, followed by 33 cycles of 30s at 94$^{o}$C, 30s at 58$^{o}$C and 1 minute at 72$^{o}$C. PCR products were electrophoresed on 1.5% agarose gels and visualized with ethidium bromide.

*Real-time quantitative PCR*

Genomic DNA was isolated from tail biopsies by proteinase K digestion, phenol/ chloroform extraction and ethanol precipitation. DNA was resuspended in TE at a concentration of 40 ng/μL. Real-time quantitative PCR was performed using a Taqman Gene Expression Assay for transferrin receptor (Tfrc) (Applied Biosystems, Foster City, CA) and a custom primer and probe set for *Gad67-SCN1A* to determine transgene copy number. The custom Taqman assay for *Gad67-SCN1A* included primers D (5' AGA CCC

CAA ACC GGT ATC ATC 3') and E (5' AGC TGT CAG GTC CTG GTG GTA 3') and probe (5'6FAM-TGC TCC ATG CGG CCG CC-MGBNFQ 3'). Real-time PCR was performed in triplicate (45 cycles) using Taqman Fast Universal PCR Master Mix on a 7900HT Fast Real-Time PCR System with Sequence Detection System 2.2 software (Applied Biosystems). All assays lacked detectable signal in no template controls. Copy number was estimated using a standard curve prepared by spiking C57BL/6J genomic DNA with *Gad67-SCN1A* plasmid DNA.

*Western blot analysis*

Western blot analysis was performed on brain membrane protein preparations that were isolated as previously described.[51] Brain membrane proteins were subjected to 7.5% SDS-PAGE and transferred to a PVDF membrane. Proteins were detected with primary antibodies directed against the HA-epitope (mouse, anti-HA.11 clone 16B12, 1:500, Covance) or the loading control β-tubulin (mouse, anti- β-tubulin clone TUB2.1, 1:5000, Sigma-Aldrich). Immunoreactive bands were detected using horseradish peroxidase-conjugated secondary antibody directed against the primary antibody (goat, anti-mouse, 1:10,000, Santa Cruz) coupled with ECL Plus reagent and then imaged with hypersensitive ECL film. Densitometry using NIH ImageJ was performed and band intensity of HA-epitope was normalized to that of β-tubulin.

*Survival Analysis*

129.*Scn1a*$^{+/-}$ females were crossed with B6.*SCN1A*$^{Tg/+}$ hemizygous males to generate F1 generation mice for a survival study. Survival was monitored until 8 weeks of age.

Littermates were used as controls. Statistical comparisons were made using the Cox proportional hazards model and $p < 0.05$ was considered statistically significant.

*Seizure threshold testing*

Flurothyl (2,2,2-trifluroethylether) was used as previously described to induce seizures in P21-24 mice.[52] Seizure threshold was determined by measuring latency to the generalized tonic-clonic seizure which is characterized by loss of posture and convulsions on the entire body. All genotypes generated from crossing 129.*Scn1a*$^{+/-}$ and B6.*SCN1A*$^{Tg/+}$ mice were used for seizure threshold testing. Statistical comparisons were made using one-way ANOVA followed by Tukey's post-test and $p < 0.05$ was considered statistically significant.

**RESULTS**

*Generation of Gad67-SCN1A mouse lines*

We generated a DNA plasmid containing the human *SCN1A* transgene. The transgene cassette includes *SCN1A* under control of the *Gad67* promoter and an IRES element preceding the fluorescent Venus (Figure 2.1). The ~2.8 kb promoter fragment from the murine *Gad1* gene includes 1.2 kb of flanking sequence, exon 1, intron 1 and 44 bp of exon 2.[53] The 6 kb human *SCN1A* cDNA construct contains 3 repeats of the HA-epitope at the C-terminus. The transgene construct was cloned into a vector containing piggyBac transposon inverted repeats. This transposon-bearing DNA plasmid and RNA encoding a transposase were microinjected into (C57BL/6J x DBA/2J)$F_1$ fertilized oocytes in the Vanderbilt University Transgenic Mouse Core. Qualitatively, *Gad67-SCN1A*

hemizygous (*SCN1A*$^{Tg/+}$) mice have no overt phenotype and are indistinguishable from wildtype littermates as they survive and breed normally. Further characterization of *Gad67-SCN1A* mice is presented below.

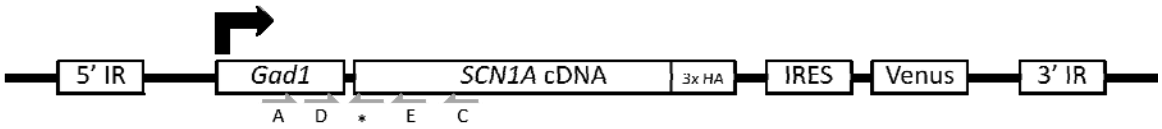


**Figure 2.1.** Structure of the *Gad67-SCN1A* transgene. Primers are indicated with half arrows. Primers A and C were used for genotyping. Primers D and E and *, probe were used for quantitative PCR.

*Gad67-SCN1A transgenic mice*

Three independent lines of mice each carrying an independent insertion of the wildtype human *SCN1A* transgene were generated. Transgenic mice were identified and the number of inserted transgene copies was estimated using real-time quantitative PCR on genomic DNA. A benefit of using the piggyBac transposon system is that transgene integration is highly efficient and it prevents the integration of concatamers.[54] The high efficiency of the piggyBac system, however, allows for multiple insertions of the transgene at different locations within the genome. Transgenic mice containing two or fewer copies of the transgene were backcrossed to C57BL/6J mice. Transgene copy number was calculated on the $N_2$ generation mice and those with a single transgene copy were selected as transgenic founders (Table 2.1).

**Table 2.1.**
*Gad67-SCN1A* transgenic lines

| Construct | Line | Copy Number | Expression |
|---|---|---|---|
| *Gad67-SCN1A* | 4.7 | 1.2 | low |
| | 9.4 | 1.0 | moderate |
| | 13.18 | 1.1 | high |
| *Gad67-SCN1A-R1648C* | 1.39 | 0.7 | not done |
| | 2.15 | 0.8 | not done |

Western blot analysis was used to determine relative transgene expression in whole brain tissue. Varying levels of the *SCN1A* transcript was detected across the three transgenic lines, with line 4.7 displaying low expression approximately 2-3 fold less abundant than line 13.18 (Figure 2.2).

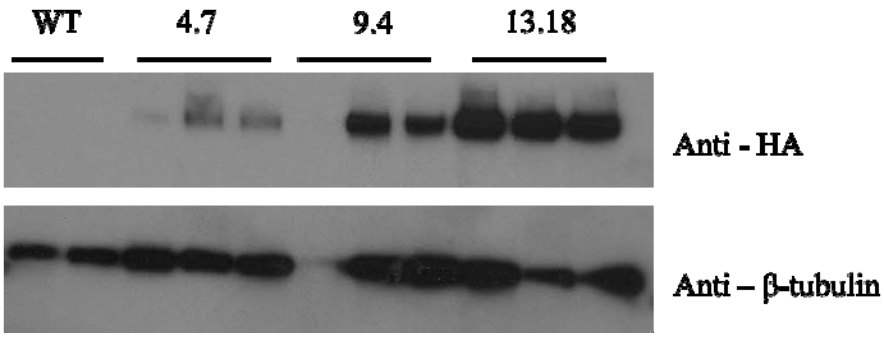


**Figure 2.2.** Western blot analysis of brain membrane proteins from *Gad67-SCN1A* transgenic lines. Representative blot for two-three biological replicates is shown for wildtype (WT) mice and mice from each of the transgenic lines. The *SCN1A* transgene was detected by antibodies directed against the HA-epitope. β-tubulin was used as a loading control. Lane 6 was mis-loaded and excluded from analysis.

In addition to the *Gad67-SCN1A* transgenic lines, we generated a transgenic line in which the Dravet syndrome associated SCN1A mutation, R1648C, is expressed selectively in GABAergic neurons (*Gad67-SCN1A-R1648C*). Two independent lines of *Gad67-SCN1A-R1648C* hemizygous mice were generated (Table 2.1). Qualitatively, transgenic mice expressing mutant *SCN1A* selectively in GABAergic neurons have no overt phenotype and a normal lifespan.

*Survival analysis of combined knockout/transgenic animals (Scn1a$^{+/-}$ :: SCN1A$^{Tg/+}$)*

*Scn1a*$^{+/-}$ mice have a significantly reduced lifespan compared to wildtype littermates with only ~25% surviving to 8 weeks of age (Figure 2.3). In order to directly test the hypothesis that the Dravet syndrome phenotype of *Scn1a*$^{+/-}$ mice can be rescued by restoring sodium channel expression selectively in inhibitory neurons, we generated combined knockout/transgenic animals (*Scn1a*$^{+/-}$ :: *SCN1A*$^{Tg/+}$) with each of the *Gad67-SCN1A* transgenic lines and monitored survival of all generated genotypes for 8 weeks. Normal survival of *Scn1a*$^{+/-}$ mice was not rescued by restoration of GABAergic *SCN1A* (Figure 2.3). *Gad67-SCN1A* transgenic line 9.4 had a trend of partial rescue but was not statistically significant ( $p = 0.059$).

*Latency to flurothyl-induced seizures*

*Scn1a*$^{+/-}$ mice exhibit a shorter latency (193 ± 21 sec) to first generalized tonic-clonic seizures following exposure to the volatile convulsant flurothyl compared to wildtype (269 ± 8 sec, $p < 0.05$) littermates. Neither *Gad67-SCN1A* transgenic line (9.4 or 13.18) was able to rescue the flurothyl-induced seizure threshold of *Scn1a*$^{+/-}$ mice.

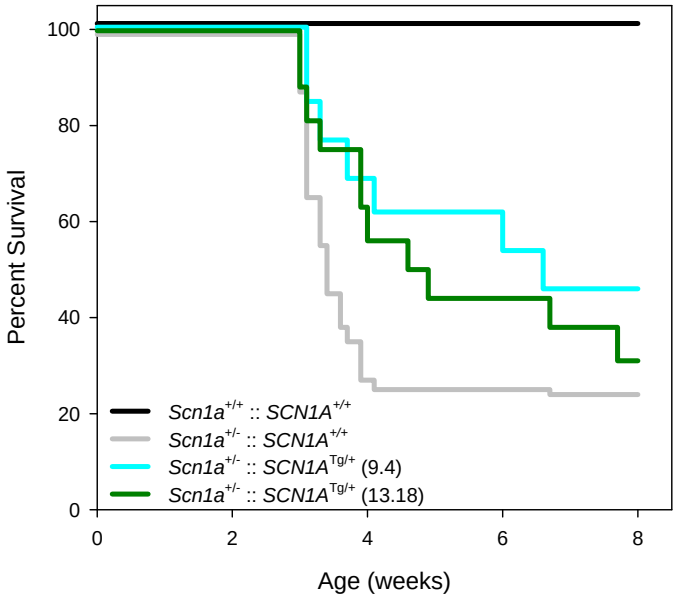


**Figure 2.3.** Survival curves of combined knockout/ transgenic mice *(Scn1a*$^{+/-}$ :: *SCN1A*$^{Tg/+}$). *Scn1a*$^{+/-}$ mice were not rescued by transgenic expression of *SCN1A* selectively in inhibitory neurons. Transgenic line is noted in parenthesis, with n = 13-55 per group. Survival difference between groups was not significant; Cox proportional hazards model.

## DISCUSSION

In an effort to determine the neurophysiological mechanism responsible for Dravet syndrome, mouse models that recapitulate the disease phenotype have been generated by targeted deletion of mouse *Scn1a* and knock-in of a human *SCN1A* truncation mutation associated with Dravet syndrome.[39,42,43] Dravet syndrome mice exhibit spontaneous seizures, premature death and a reduced threshold for induced seizures. Electrophysiological recordings from *Scn1a*$^{+/-}$ mouse hippocampal neurons have shown reduced sodium current density and excitability of GABAergic interneurons, which is hypothesized to be the basis for Dravet syndrome. More recent studies have generated mice in which *SCN1A* has been conditionally knocked-out of inhibitory neuron populations. Conditional deletion of *Scn1a* from interneurons was sufficient to cause

epilepsy and lethality in mice.[50] Results from these mouse models support the interneuron-hypothesis of epileptogenesis in Dravet syndrome.

We hypothesized that restoration of *SCN1A* selectively in interneurons would attenuate or prevent the epilepsy phenotype in Dravet syndrome mice, and generated a *Gad67-SCN1A* transgenic mouse line that expresses human *SCN1A* selectively in GABAergic neurons. Experiments with combined knockout/transgenic mice are still ongoing. Preliminary experiments, however, show that selective expression of *SCN1A* in inhibitory neurons of *Scn1a*$^{+/-}$ mice was not able to rescue the Dravet syndrome phenotype. While one *Gad67-SCN1A* line (9.4) showed a trend of partial rescue for the survival of *Scn1a*$^{+/-}$ mice, the improvement was not statistically significant. The survival study was greatly under-powered (power = 0.4) to observe partial rescue as we had assumed full rescue during experimental design. In order to achieve statistical significance, sample size would need to increase 3-fold. Additionally, no improvement was observed with either *Gad67-SCN1A* transgenic line for the reduced threshold to flurothyl-induced seizures in *Scn1a*$^{+/-}$ mice. Our preliminary results are not entirely consistent with the idea of an interneuron-only defect in Dravet syndrome as the cause of premature mortality and suggest the possibility of an additional mechanism. This is consistent with recent work proposing that a combination of both inhibitory interneuron and excitatory pyramidal neuron dysfunction contributes to the lethality of Dravet syndrome in mice. Studies in acutely dissociated hippocampal neurons isolated from *Scn1a*$^{+/-}$ mice revealed increased sodium current density and a hyperpolarized shift in the voltage-dependence of activation of pyramidal neurons compared to wildtype littermates in addition to reduced sodium

current density in inhibitory GABAergic interneurons.[44] Additionally, increased sodium current density was observed in pyramidal neurons differentiated from Dravet syndrome patient-derived iPSCs.[55] This idea of a hyperexcitable component to the pathology of Dravet syndrome is further explored in Chapter III.

We were not able to attenuate or prevent the premature death phenotype of *Scn1a*$^{+/-}$ mice by restoring *SCN1A* selectively in GABAergic neurons using *Gad67-SCN1A* transgenic mouse lines. We have suggested that the failure of the *Gad67-SCN1A* mouse lines to rescue survival in *Scn1a*$^{+/-}$ mice may be because additional mechanisms underlie the pathophysiology of Dravet syndrome rather than only a loss of GABA-mediated inhibition. Other possible reasons for this failure may relate to the transgene integration site into the genome, or the cellular localization of the transgene product. If the transgene inserted within an essential gene, this could confound our results. It is also possible that we failed to observe rescue due to the targeting of all *Gad67* positive (*Gad67*+) neurons. While *Gad67* expression marks GABA producing neurons, GABAergic lineages are divided into interneuron populations that project locally and neuron populations with long-range projections. By using the *Gad67* promoter to drive sodium channel expression, the rescue strategy also includes *Gad67*+ non-interneurons which may be affecting rescue. Additionally, it is known that interneurons innervate and control other interneurons.[56,57] Because our rescue strategy for restoring *SCN1A* expression included all *Gad67*+ neurons, it is possible that interneuron/interneuron interactions became overactive, leading to a resultant hyperexcitability of the hippocampus. To address these concerns, future experiments should restore *SCN1A* expression in specific interneuron

subpopulations such as parvalbumin- or somatostatin-positive inhibitory interneurons. Another possibility explaining why the *Gad67-SCN1A* transgenic lines did not rescue the phenotype could be because we either restored too much or failed to achieve adequate sodium channel expression. To address this concern, we propose electrophysiological experiments to examine sodium current density in acutely dissociated hippocampal interneurons from each of the transgenic lines because we found that they have varying levels of transgene expression.

In some cases of Dravet syndrome, conventional sodium channel-blocking antiepileptic drugs (AEDs) such as lamotrigine have been shown to paradoxically worsen the disease.[58] There are currently no models in which AED-induced exacerbation of epilepsy has been replicated. *In vitro*, our lab has shown that lamotrigine treatment increases cell surface expression of the Dravet syndrome associated *SCN1A* mutation R1648C.[35] Functional characterization of *SCN1A-R1648C* has revealed both gain- and loss-of-function phenotypes. *SCN1A-R1648C* exhibits persistent sodium current in addition to an overall reduced sodium current density resulting from impaired cell surface trafficking.[31,35] Lamotrigine treatment rescues cell surface trafficking of *SCN1A-R1648C* which evokes increased persistent sodium current that could exacerbate seizure generation. In order to examine the underlying mechanism responsible for the worsening phenotype of Dravet syndrome patients treated with certain AEDs, we generated a transgenic mouse line in which *SCN1A-R1648C* was expressed selectively in GABAergic neurons (*Gad67-SCN1A-R1648C*). We will use this mouse line to investigate trafficking

rescue of a dysfunctional channel as a potential mechanism for the exacerbation of the Dravet syndrome phenotype by some AEDs.

CHAPTER III

# PREFERENTIAL INHIBITION OF PERSISTENT SODIUM CURRENT IS AN EFFECTIVE ANTIEPILEPTIC DRUG MECHANISM

## INTRODUCTION

Epilepsy is a common neurological disorder characterized by recurrent, spontaneous seizures.[1-3] Antiepileptic drugs (AEDs) are the mainstay of treatment for most patients and several mechanistically distinct classes of agents are available. Unfortunately, 30% of persons affected by epilepsy fail to achieve adequate seizure control with currently available pharmaceuticals suggesting the need for new AEDs.[3]

Many widely used and successful AEDs target voltage-gated sodium ($Na_v$) channels, typically by mechanisms resulting in use-dependent block of transient sodium current. Persistent sodium current, a small non-inactivating component of overall current carried by $Na_V$ channels, may be another potential target for AED action. Neurons in several brain regions exhibit persistent sodium current and this activity may help amplify subthreshold synaptic potentials and facilitate repetitive firing.[59] Further, increased persistent sodium current is an observed feature of several heterologously expressed mutant human $Na_v$ channels associated with familial epilepsy syndromes such as genetic epilepsy with febrile seizures plus (GEFS+).[60] Ranolazine is an FDA-approved drug for the treatment of angina pectoris arising from coronary insufficiency and acts by preferentially inhibiting persistent sodium current in heart. We previously reported that

ranolazine can suppress persistent current generated by several human $Na_V1.1$ mutations associated with genetic epilepsies or familial hemiplegic migraine.[61] Ranolazine has also been shown to reduce action potential firing and epileptiform activity in cultured neurons.[62] Whether preferential suppression of persistent sodium current would be antiepileptic *in vivo* is unknown.

The genetically engineered mouse line, *Scn2a*$^{Q54}$, expresses a transgene encoding an inactivation-impaired neuronal $Na_V1.2$ channel. Mice expressing the *Scn2a*$^{Q54}$ transgene exhibit a severe epilepsy phenotype that is characterized by short-duration partial seizures beginning in early life that then progress to secondarily generalized seizures, status epilepticus and premature death.[40,41] Epilepsy in *Scn2a*$^{Q54}$ mice is correlated with increased persistent sodium current in hippocampal neurons. These animals also exhibit histopathologic changes in the hippocampus, including hilar neuron loss and mossy fiber sprouting that also occur in chronic human epilepsy. This animal model provides an excellent opportunity to test the efficacy of drugs targeting persistent sodium current. We hypothesized that preferential inhibition of persistent sodium current would eliminate sodium channel dysfunction and exert an antiepileptic effect in *Scn2a*$^{Q54}$ mice.

Heterozygous *Scn1a* knockout (*Scn1a*$^{+/-}$) mice exhibit a severe epilepsy phenotype with spontaneous seizures and premature death that models Dravet syndrome in humans. Heterozygous loss of *Scn1a* impairs GABA-mediated inhibition because of a reduced sodium current density and neuronal excitability in GABAergic interneurons.[42-44] Due to the haploinsufficiency of *SCN1A*, it should come as no surprise that conventional

voltage-gated sodium channel blockers are ineffective in patients with Dravet syndrome. In some cases, lamotrigine has even been shown to cause a paradoxical worsening of the disease.[58] We hypothesized that *Scn1a*$^{+/-}$ mice would either be resistant to or would exhibit seizure aggravation with drugs targeting persistent sodium current.

In this study, we investigated the antiepileptic effect of preferential persistent sodium current inhibition using ranolazine and the recently described novel compound, GS967.[63,64] We observed that both ranolazine and GS967 reduced seizure frequency in *Scn2a*$^{Q54}$ mice, and GS967 inhibited spontaneous action potential firing in neurons isolated from *Scn2a*$^{Q54}$ mice. GS967 was also effective at protecting against seizures in the maximal electroshock (MES) model. Additionally, we found that long-term treatment with GS967 greatly improved survival, prevented hilar neuron loss and suppressed the development of mossy fiber sprouting in *Scn2a*$^{Q54}$ mice. Surprisingly, we also found that survival of *Scn1a*$^{+/-}$ mice was significantly improved with long-term treatment of GS967.

## MATERIALS AND METHODS

### *Animals*

All animal care and experimental procedures were approved by the Vanderbilt University Institutional Animal Care and Use Committee. Mice were group-housed in a pathogen-free mouse facility under standard laboratory conditions (12-h light/dark cycle). Mice had access to food and water *ad libitum*, except during experiments. *Scn2a*$^{Q54}$ transgenic mice were generated as previously described and are maintained as a congenic line on the

C57BL/6J background (B6.Q54) by continued backcrossing of B6.Q54 hemizygous males to C57BL/6J females.[40] For experiments, F1 generation *Scn2a*$^{Q54}$ mice were produced by crossing B6.Q54 hemizygous transgenic males with SJL/J females. *Scn1a*$^{+/-}$ mice were generated as previously described and are maintained as a congenic line on the 129S6/SvEvTac background (129.*Scn1a*$^{+/-}$).[43] For experiments, F1 generation *Scn1a*$^{+/-}$ mice were produced by crossing 129.*Scn1a*$^{+/-}$ mice with C57BL/6J mice. Mice were tail biopsied in the second postnatal week, and DNA was prepared from tail tissue using Gentra Puregene Mouse Tail kit according to the manufacturer's instructions (Qiagen, Valencia, CA). Genotyping of the *Scn2a*$^{Q54}$ transgene was performed as previously described.[41] Genotyping of *Scn1a*$^{+/-}$ mice was performed as previously described.[43] Experimental animals used in this study were age 30-35 days unless otherwise noted.

*Drugs and compounds*

Ranolazine dihydrochloride (Sigma-Aldrich, St. Louis, MO, USA), phenytoin sodium injection, USP (Baxter Healthcare, Corp., Deerfield, IL, USA), phenytoin (Sigma-Aldrich, St. Louis, MO, USA) and GS967 (Gilead Sciences, Foster City, CA, USA) were used. For electrophysiological experiments, phenytoin and GS967 were prepared at stock concentrations of 50 mM and 10 mM respectively in DMSO, and diluted in the appropriate bath solution at the time of recording. The final DMSO concentration was always less than 0.02%. A solution of ranolazine was prepared in Dulbecco's phosphate buffered saline (PBS) with pH readjusted to 7.1. Drug-free PBS was used as a vehicle control for ranolazine experiments. Phenytoin sodium was diluted in 0.5% methyl cellulose, and the vehicle control solution contained 10% ethyl alcohol, 40% propylene

glycol and 50% water diluted in 0.5% methyl cellulose. The pH of phenytoin and vehicle solutions was between 7.5 and 8.0. A solution of GS967 was prepared in a vehicle solution containing 15% NMP, 10% solutol HS-15 and 75% water for MES experiments. GS967 was formulated in Purina 5LOD chow at concentrations of 2 mg/kg and 8 mg/kg by Research Diets, Inc. for experiments involving *Scn2a*$^{Q54}$ and *Scn1a*$^{+/-}$ mice.

*In vivo pharmacology*

Non-transgenic F1 wildtype (C57BL/6J x SJL/J) mice purchased from The Jackson Laboratory (Bar Harbor, ME, USA) were used to study ranolazine pharmacokinetics *in vivo*. Ranolazine (40 mg/kg) was administered as a single intraperitoneal (i.p.) injection in a volume of 10 ml/kg body weight. At selected time points (10, 20, 30 or 40 minutes), four animals per group were deeply anesthetized before collecting blood and brain samples. Blood and brain samples were also collected from the phenytoin and GS967 experimental animals. Plasma was isolated by centrifugation (9000 x g, 10 minutes). Brain tissue was homogenized in 3% sodium fluoride solution containing 1% HCl (300 mg tissue in 600 µl). Ranolazine and GS967 concentrations were measured by liquid chromatography coupled with tandem mass spectrometry as previously described.[61] Plasma phenytoin concentration was assayed by Vanderbilt University Medical Center Core Chemistry Laboratory using fluorescence polarization immunoassay technology (COBAS INTEGRA; Roche, Basel, Switzerland).

*Acute isolation of hippocampal neurons*

Electrophysiology experiments were performed on acutely dissociated hippocampal pyramidal neurons isolated from *Scn2a*$^{Q54}$ mice. Mice were anesthetized with isoflurane and brains were removed under aseptic conditions. Slices (400 μm) were obtained using a Leica VT1200 microtome (Leica Microsystems, Nussloch, Germany). The hippocampus was isolated by dissection in ice cold sterile filtered dissection solution (in mM: 110 NaCl, 2.5 KCl, 7.5 $MgCl_2$, 10 HEPES, 75 sucrose, 25 glucose, pH 7.4), then allowed to recover in ACSF solution containing (in mM: 124 NaCl, 4.4 KCl, 2.4 $CaCl_2$, 1.3 $MgSO_4$, 1 $NaH_2PO_4$, 10 glucose, and 26 $NaHCO_3$, pH 7.35) for a period of 1-6 hours. Neurons were dissociated by protease XXIII digestion (1.5 mg/ml) at room temperature in a solution containing (in mM: 82 $Na_2SO_4$, 30 $K_2SO_4$, 5 $MgCl_2$, 10 HEPES, 10 glucose, pH 7.4). Cells were triturated in dissociation solution containing 1 mg/ml bovine serum albumin, then placed in recording solution for electrophysiological experiments.[65]

*Electrophysiology*

Mutagenesis of recombinant rat $Na_V1.2$ ($rNa_V1.2$) was performed as described previously.[26,66,67] Three mutations (G879Q, A880Q, L881Q) were introduced into full length $rNa_V1.2$ to recapitulate the *Scn2a*$^{Q54}$ transgene. Heterologous expression of $rNa_V1.2$ in tsA201 cells and whole cell voltage clamp recording were performed as previously described.[68] Persistent sodium current was measured during the final 10 ms of a 200 ms depolarization to −10 mV from a holding potential of −120 mV in the absence and presence of 1 μM GS967 or 10 μM phenytoin, followed by application of 0.5 μM tetrodotoxin (TTX) and offline digital subtraction as described previously.[68] Use-

dependent rundown was measured at stimulation frequencies of 10, 30, and 100 Hz in the absence and presence of either 1 μM GS967 or 10 μM phenytoin, followed by application of 0.5 μM TTX and offline digital subtraction of TTX-resistant current. Whole cell recordings of neuronal cell bodies were made in current clamp mode using an Axon MultiClamp 700B amplifier. Patch pipettes were fabricated from borosilicate glass using a multistage P-97 Flaming Brown micropipette puller (Sutter Instruments, Novato, CA), and fire-polished using a microforge (Narishige, Japan). Final pipette resistance was 2.0 – 2.5 MΩ when filled with a solution containing (in mM: 110 K-gluconate, 10 KCl, 10 HEPES, 10 dextrose, 10 sucrose, 10 phosphocreatine-$Na_2$, 5 EGTA, 4 Mg-ATP, 0.3 Na-GTP, 0.1 $CaCl_2$, pH 7.35, 300 mOsmol/kg). Bath solution consisted of (in mM: 155 NaCl, 3.5 KCl, 1 $MgCl_2$, 1.5 $CaCl_2$, 10 HEPES, pH 7.35). The reference electrode consisted of a 2% agar bridge with composition of the bath solution. All whole-cell recordings were low-pass Bessel filtered at 5 kHz and digitized at 50 kHz. Membrane potential was clamped to −80 mV and cells were allowed to fire spontaneously. Spontaneous action potential firing frequency was measured in the absence and presence of GS967 (100, 300 and 1000 nM). Statistical comparisons were made using either Student's t-test or one-way ANOVA followed by Tukey's post-test and $p < 0.05$ was considered statistically significant.

*Evaluation of anti-seizure activity in Scn2a$^{Q54}$ mice*

Anti-seizure activity was evaluated by comparing the number of behavioral seizures captured by video recording during a 30-min pre-treatment period with the number occurring during a 30-min post-drug period in male *Scn2a*$^{Q54}$ mice. Behavioral seizures

(tonic deviation of the head and body accompanied by forelimb clonus) were previously correlated with electroencephalographic seizures using video-EEG monitoring, and work in our laboratory has shown strong agreement between detection of seizures using behavioral and electroencephalographic observations (kappa 0.988) in untreated mice.[40] Mice were implanted with prefabricated headmounts (Pinnacle Technology, Inc., Lawrence, KS, USA) for video-EEG monitoring as previously described.[52]Video-EEG data was collected from ranolazine treated mice. Mice were placed in individual clear Plexiglas recording cages for 60-min prior to drug treatment (30-min habituation followed by the 30-min pre-treatment period). Drug treatments were randomly assigned within experimental groups. Mice received 40 mg/kg ranolazine (maximum tolerated dose) or PBS as a single i.p. injection and were immediately returned to the recording cage for the 30-min post-treatment period. Phenytoin experimental animals received a single i.p. injection of either 30 mg/kg phenytoin, which produced a plasma concentration within the human therapeutic range, or vehicle and were returned to the home cage for a delay of 75-min. Mice were then placed into the recording cage for 30-min habituation followed by the 30-min post-treatment period. The delay between drug injection and post-treatment period for each drug was based upon the time to peak plasma ranolazine concentration and the previously determined time to peak phenytoin effect.[69] For both ranolazine and phenytoin experiments, digital video images captured during the two 30-min video-monitored periods (pre- and post-drug treatment) were analyzed offline by two independent observers blinded to treatment. Statistical comparisons were made using repeated measures ANOVA and $p < 0.05$ was considered statistically significant.

GS967 could not be administered satisfactorily by the i.p. route because the vehicle alone caused excessive sedation in mice, and the stress of intravenous or oral gavage administration would have exacerbated seizures in *Scn2a*$^{Q54}$ mice. Therefore, GS967 was administered orally through supplementation in chow. Baseline seizure frequency was quantified for 30 minutes in the GS967 experimental group (pre-treatment period), then mice were returned to the home cage and received either control or GS967 containing chow (either 2 mg drug per kg chow or 8 mg drug per kg chow; dosage estimated as 0.375 mg/kg/d and 1.5 mg/kg/d, respectively, based on the consumption of 3.5-4 g chow per day). Seizures were quantified offline by two independent observers blinded to treatment for 30 minutes at 24 and 48 hours after onset of treatment (post-treatment period), and percent change in seizure frequency was calculated. Statistical comparisons were made using repeated measures ANOVA and $p < 0.05$ was considered statistically significant.

*Maximal electroshock-induced seizures*

MES experiments were performed at The Jackson Laboratory (Bar Harbor, ME, USA) using 9 week old C57BL/6J male mice. Mice were administered either GS967 or phenytoin solutions by oral gavage in a volume of 10 ml/kg body weight 2 hours prior to MES testing. All tests were conducted at the empirically determined time to peak GS967 and previously determined time to peak phenytoin effect.[69] Transcorneal electrodes were placed on anesthetized corneas (0.5% tetracaine in normal saline). Electrical stimuli (20.5 mA, 299 Hz, 1.6 ms pulse width, constant current previously determined to be the critical current for 97% of C57BL/6J animals to experience tonic hindlimb extension was

delivered for 0.2s using the Ugo Basile (Model 7800) electroconvulsive device (Stoelting Co., Wood Dale, IL, USA).[70] Maximal seizures appear as a tonic-clonic flexion/extension sequence, beginning with tonic extension of the forelimbs and terminating with tonic hindlimb extension. Maximal seizures were scored with full tonic hindlimb extension (hindlimbs at 180 degree angle to the torso) as the endpoint. Probit analysis was used to determine $ED_{50}$ values (concentration required to protect 50% of animals against MES-induced seizures) for GS967 and phenytoin.

*Survival Analysis*

At weaning (postnatal day 21), *Scn2a*$^{Q54}$ mice were randomly assigned to either GS967 or control treatment groups. Survival was monitored until 12 weeks of age. *Scn1a*$^{+/-}$ mice were weaned at postnatal day 18 and randomly assigned to either GS967 or control treatment groups. Survival was monitored until 8 weeks of age. Animals in the GS967 treatment group were provided chow containing GS967 (8 mg/kg). Statistical comparisons were made using the Cox proportional hazards model and $p < 0.05$ was considered statistically significant.

*Histology*

Cresyl Violet and Timm staining were used to detect hilar neuron loss and mossy fiber sprouting, respectively, in the dentate gyrus of female mice (age 60-65 days). At weaning (postnatal day 21), *Scn2a*$^{Q54}$ mice or wildtype (WT) littermates were randomly assigned to either GS967 or control treatment groups. Animals in the GS967 experimental group were provided chow containing GS967 (8 mg/kg) until morning of

sacrifice. Mice in both treatment groups underwent 30 minutes of video-taped observation just before sacrifice. Seizure frequency was quantified by offline analysis of the video recordings by an observer blinded to treatment. Staining with Cresyl Violet was performed as previously described.[40] Timm staining was performed as previously described.[71] Mossy fiber sprouting was measured by quantifying the density of stain within the inner molecular layer of the dentate gyrus from both the suprapyramidal and infrapyramidal blades. An image of the dentate gyrus was obtained with a 10x objective from 2 sections from each mouse. NIH ImageJ was used to acquire a total of 6 density measurements from each section (12 measurements per mouse). Each measurement was normalized to the background staining within the outer molecular layer of the section (Figure 3.1). These values were averaged to obtain a single density measurement for each animal. Mossy fiber sprouting was compared among groups using one-way ANOVA followed by Tukey HSD post-hoc tests and $p < 0.05$ was considered statistically significant. Statistical analysis was conducted using STATA 12.0 (StataCorp LP, College Station, TX).

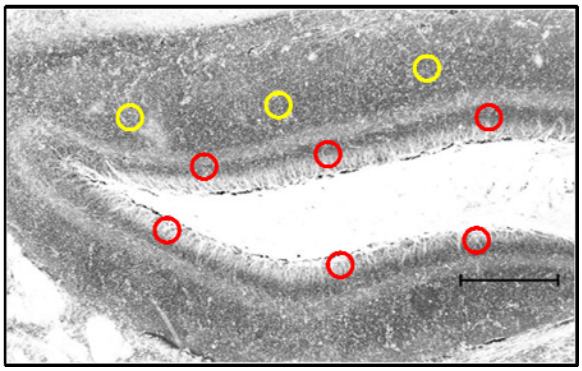

**Figure 3.1.** Quantification strategy for mossy fiber sprouting. NIH ImageJ was used to perform densitometry within the granular layer of the dentate gyrus. Density measurements were made within the inner molecular layer of the dentate gyrus from both the suprapyramidal and infrapyramidal blades (red circles). Each measurement was normalized to the average background staining within the outer molecular layer of the section (yellow circles). Areas measured were circles with a radius of 0.36 inches.

## RESULTS

*Ranolazine reduces seizure frequency in Scn2a$^{Q54}$ mice*

Previous work in heterologous cells demonstrated that ranolazine preferentially suppressed persistent sodium current induced by several human $Na_V1.1$ mutants.[72] Here we tested the ability of ranolazine to reduce seizure frequency *in vivo* using *Scn2a*$^{Q54}$ mice that have seizures as a consequence of an abnormal neuronal persistent sodium current conducted by a mutant $Na_V1.2$ transgene. Seizure frequency was quantified for 30 minutes before and after intraperitoneal administration of 40 mg/kg ranolazine or vehicle. Ranolazine reduced seizure frequency significantly compared to vehicle treated animals (Figure 3.2). Additionally, a subset of animals (n=9) were monitored with simultaneous video-EEG recording. Following acute ranolazine treatment, we found a 98% correlation between electroencephalographic and behavioral seizures (55 behavioral vs 56 electroencephalographic) and this was not different from untreated animals. The proportional reduction in seizure frequency was modest (48%) possibly due to short plasma half-life (~15 minutes) and low brain penetration of ranolazine in mice (Table 3.1). Despite the pharmacokinetic limitations of ranolazine, these results provided a proof-of-principle that preferential suppression of persistent sodium current can exert an antiepileptic effect.

**Table 3.1.**
Plasma and brain concentrations

| Drug* | Dosage (mg/kg)** | % Change in Seizure Frequency | [Plasma]† | [Brain] |
|---|---|---|---|---|
| Ranolazine | 40 | -48 ± 10% | 19.3 ± 0.8 μM | 4.9 ± 0.1 μM |
| Phenytoin | 30 | -93 ± 5% | 87.2 ± 1.2 μM | ND |
| GS967 | 1.5 | -92 ± 4% | 0.6 ± 0.1 μM | 0.6 ± 0.2 μM |

*Ranolazine and phenytoin were administered as single i.p. injections. GS967 was orally administered through supplementation in chow. **, GS967 dose is in units of mg/kg/day; †phenytoin and GS967 are both highly (>90%) protein bound in plasma; ND, not determined

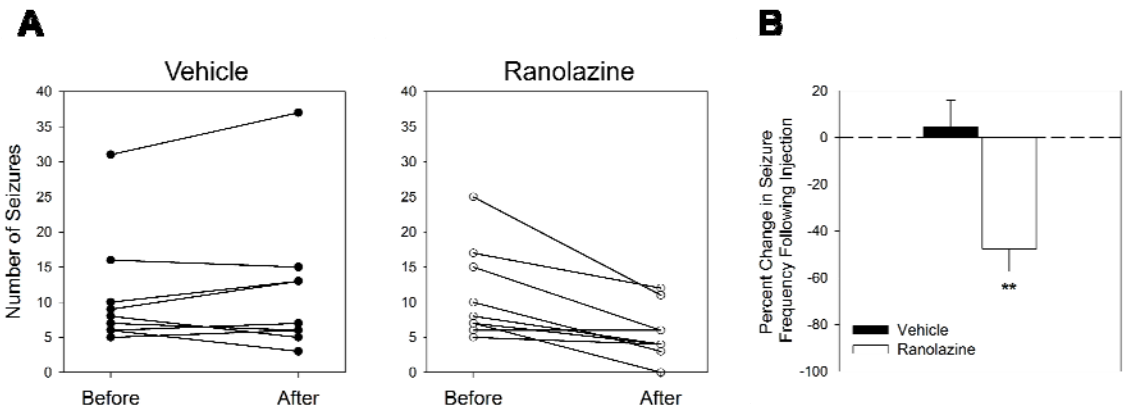


**Figure 3.2.** Ranolazine reduces seizure frequency in *Scn2a*$^{Q54}$ mice. (**A**) Number of seizures for individual male mice before and after treatment of either vehicle (*left*) or ranolazine (*right*). (**B**) A histogram of percent change in seizure frequency following a single i.p. injection of either vehicle or ranolazine (40 mg/kg). Percent change was calculated in response to treatment, with n = 9 for each treatment (**$p$ < 0.005; repeated measures ANOVA).

*GS967 inhibits persistent current and spontaneous action potential firing*

The novel compound, GS967, has recently been shown to selectively inhibit persistent sodium current mediated by the cardiac voltage gated sodium channel with much greater potency than ranolazine and has no cross reactivity with over 600 other molecular targets at 1 μM concentration.[63] To investigate the effects of GS967 on brain $Na_V$ channels, we performed whole-cell voltage clamp recordings on tsA201 cells expressing a mutant $Na_V1.2$ cDNA derived from the *Scn2a*$^{Q54}$ transgene ($Na_V1.2$-GAL879-881QQQ). External application of GS967 suppressed persistent sodium current with an estimated $IC_{50}$ of 0.44 ± 0.16 μM, while peak (transient) current was inhibited with an estimated $IC_{50}$ of 18.7 ± 47.2 μM (solubility limits of GS967 precluded testing concentration higher than 10 μM) indicating a 42-fold greater preference for persistent current block over peak current block ($p$ < 0.05; Figure 3.3 A,C). For comparison, phenytoin, a commonly prescribed AED, also inhibited persistent current ($IC_{50}$ of 15.9 ± 24.7 μM vs. $IC_{50}$ of

143.7 ± 70.1 μM, $p < 0.05$; Figure 3.3 B,C), but with lower potency and less preference (9-fold) over peak compared to GS967. Additionally, application of 1 μM GS967 induces small hyperpolarized shifts in the voltage dependence of activation and steady-state inactivation, and slows the fast component of recovery from fast inactivation (Figure 3.4, Table 3.2). A common feature of several AEDs is use-dependent inhibition of transient sodium current. Therefore, we examined use-dependent inhibition of $Na_V1.2$-GAL879-881QQQ mediated sodium current by either 1 μM GS967 or 10 μM phenytoin at different frequencies (10 – 100 Hz). We observed minimal steady-state use-dependent inhibition by GS967 across the range of stimulation frequencies (Figure 3.3 D), consistent with the activity of this drug observed on the cardiac voltage gated sodium channel.[63] However, as expected, phenytoin exhibited strong use-dependent block of transient sodium current (Figure 3.3 D), with a greater degree of inhibition at high stimulation frequencies (44.2 ± 3.7%) compared to low frequency stimulation (22.6 ± 2.8%, $p < 0.05$). These data suggest that GS967 acts mainly through a tonic block mechanism to preferentially inhibit persistent sodium current.

**Table 3.2.**

Effect of GS967 on $Na_v1.2$-GAL978-881QQQ Biophysical Properties

| | Voltage Dependence of Activation | | Voltage Dependence of Fast Inactivation | | Recovery from Fast Inactivation | |
|---|---|---|---|---|---|---|
| | $V_{1/2}$ (mV) | k (mV) | $V_{1/2}$ (mV) | k (mV) | $\tau_f$ (ms) | $\tau_s$ (ms) |
| Control | -15.2 ± 0.8 | 8.5 ± 0.2 | -67.5 ± 1.4 | -5.4 ± 0.1 | 7.3 ± 0.5 (84 ± 2%) | 572.1 ± 81.6 (17 ± 4%) |
| GS967 | -18.1 ± 0.9* | 8.6 ± 0.2 | -71.1 ± 1.6* | -5.5 ± 0.2 | 15.2 ± 3.2* (40 ± 5%*) | 78.9 ± 8.5* (56 ± 4%*) |

*$p < 0.05$ compared to control conditions, with n = 9-15 per condition

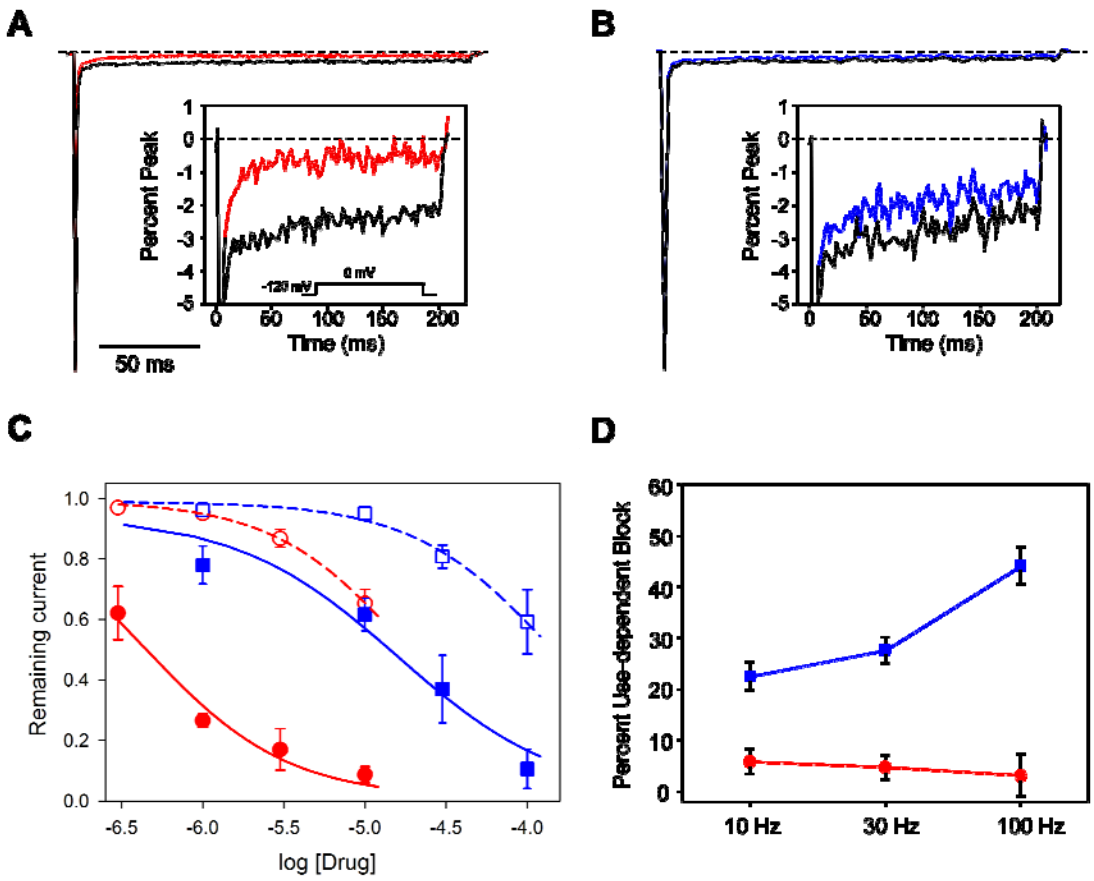


**Figure 3.3.** GS967 inhibits persistent sodium current. **(A)** Representative trace of sodium current in the absence (black trace) or presence (red trace) of 1 μM GS967. The inset illustrates persistent sodium current on an expanded scale. **(B)** Representative trace of voltage dependent sodium current in the absence (black trace) or presence (blue trace) of 10 μM phenytoin. The inset illustrates persistent sodium current on an expanded scale. **(C)** Concentration response inhibition of persistent sodium current (closed symbols, solid lines) and transient sodium current (open symbols, dashed lines) by GS967 (red circles) and phenytoin (blue squares). **(D)** Steady-state use-dependent inhibition of transient sodium current by either 1 μM GS967 (red symbols) or 10 μM phenytoin (blue symbols) at stimulation frequencies of 10, 30, or 100 Hz. Values represent ratios of use-dependent inhibition in the presence of drug to that in the absence of drug. All data are expressed as mean ± SEM, with n = 7-11 for each condition – Chris Thompson, PhD.

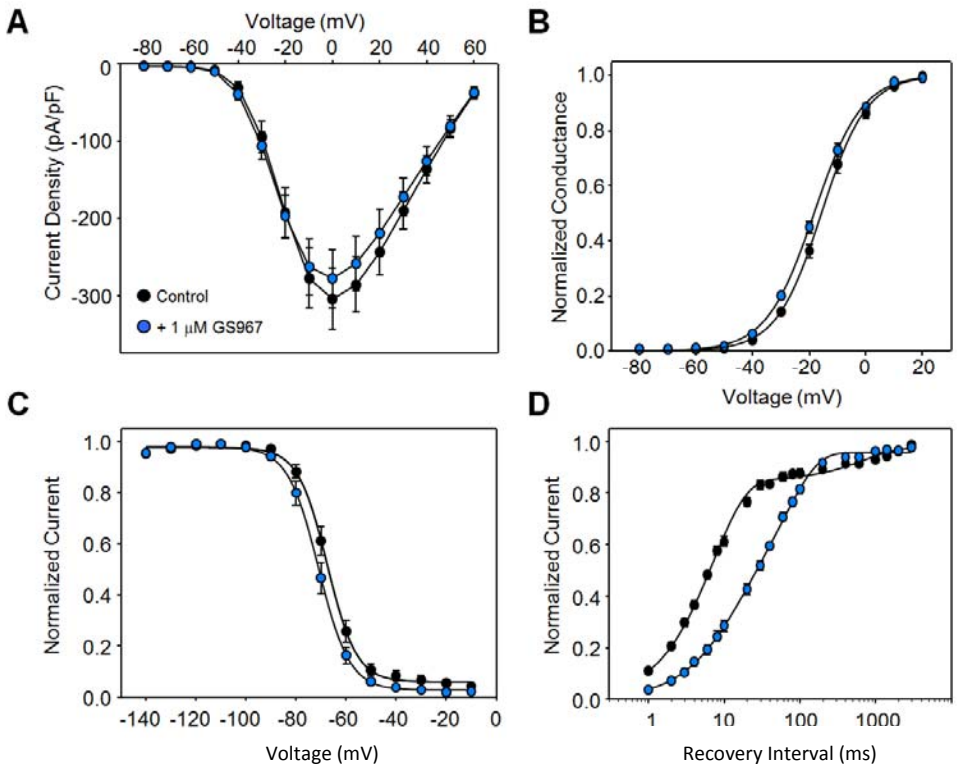


**Figure 3.4.** Effect of GS967 on $Na_V1.2$-GAL879-881QQQ biophysical properties. **(A)** Peak current density elicited by test pulses to various membrane potentials and normalized to cell capacitance. **(B)** Voltage dependence of channel activation measured between −80 to +20mV **(C)** Voltage dependence of inactivation measured following a 100 ms inactivating prepulse ranging from −140 to −10 mV. **(D)** Time-dependent recovery from inactivation assessed with a 100 ms inactivating prepulse to −10 mV. Black symbols represent data recorded under control conditions while blue symbols are data recorded in the presence of 1 μM GS967. Data are represented as mean ± S.E.M., with n = 9 – 11 for each condition – Chris Thompson, PhD.

We next investigated whether GS967 could exert preferential suppression of persistent sodium current in neurons isolated from *Scn2a*$^{Q54}$ mice and whether this effect would inhibit neuronal action potential firing. Persistent current measurements from hippocampal pyramidal neurons isolated from *Scn2a*$^{Q54}$ mice demonstrated that 1 μM GS967 significantly reduced persistent current from 1.2 ± 0.4% of peak current amplitude (n = 8) measured under control conditions to 0.1 ± 0.1% (n = 5, $p < 0.05$; Figure 3.5 A,B). Whole-cell current clamp recording was then performed on hippocampal pyramidal

neurons in the presence and absence of GS967. Neurons isolated from *Scn2a*$^{Q54}$ mice exhibited high frequency spontaneous action potential firing, unlike wildtype littermates that exhibit rare spontaneous firing (Figure 3.5 C). Application of 1 μM GS967 reduced firing frequency by 98.8 ± 0.1% (n = 7) and this effect was reversible upon washout of the compound. Suppression of neuronal firing by GS967 was concentration-dependent, with an estimated $IC_{50}$ of ~250 nM (Figure 3.5 D). By comparison, 1 μM phenytoin inhibited spontaneous action potential firing by only 36.7 ± 10.1% (open square in Figure 3.5 D).

Based on these *in vitro* observations coupled with the ability of GS967 to effectively cross the blood-brain barrier (Table 3.1), and a slower rate of elimination than ranolazine, we hypothesized that GS967 would exert antiepileptic activity *in vivo.* Accordingly, we examined the effect of GS967 *in vivo* using three distinct mouse models of epilepsy.

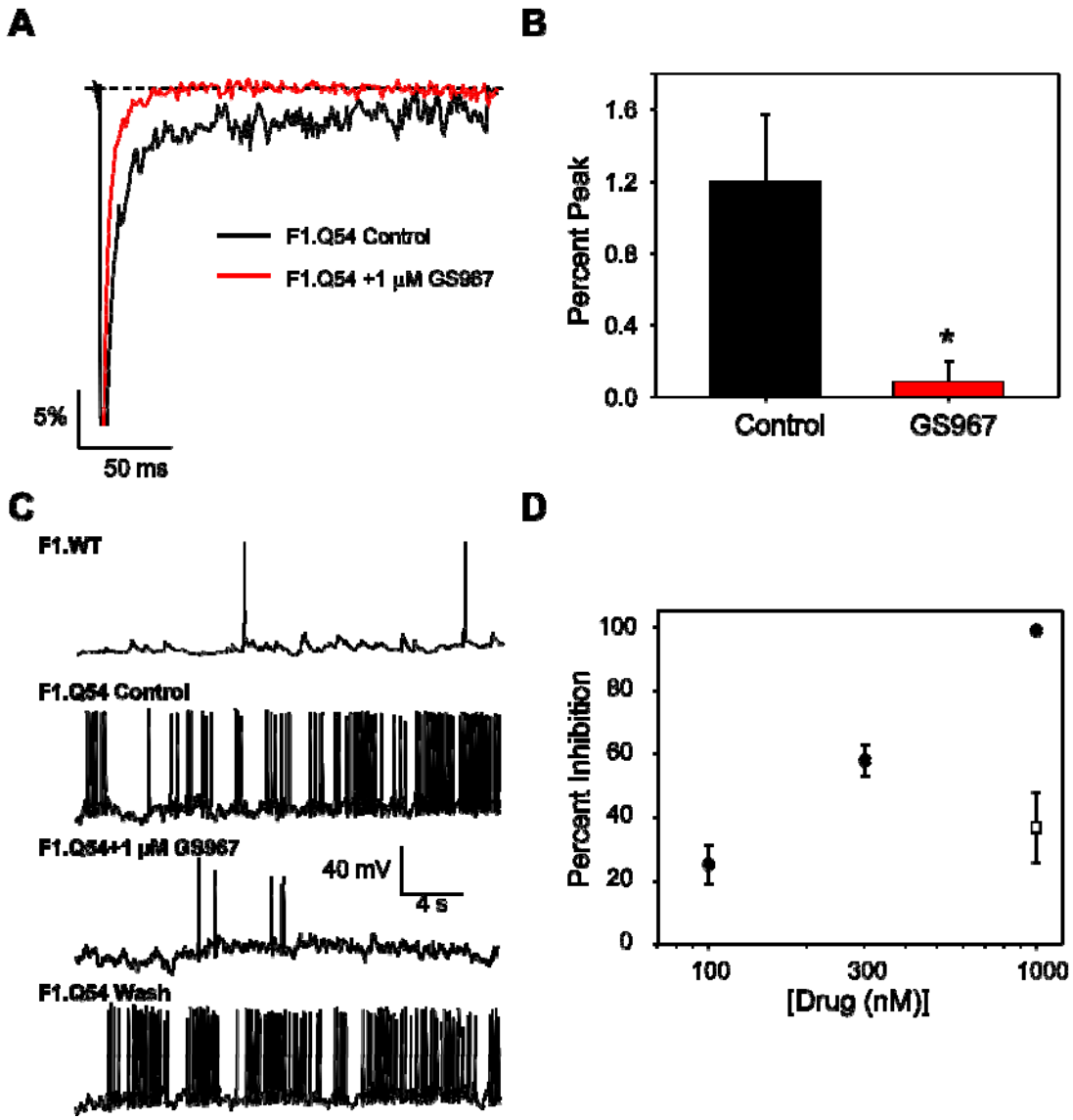


**Figure 3.5.** GS967 inhibits persistent current and spontaneous firing in *Scn2a*$^{Q54}$ neurons. **(A)** Representative normalized trace of sodium currents from hippocampal pyramidal neurons from *Scn2a*$^{Q54}$ (F1.Q54) mice recorded in the absence (black trace) or presence (red trace) of 1 µM GS967. (**B**) Summary data for persistent sodium current (expressed as % of peak current) recorded from pyramidal neurons in the absence or presence of 1 µM GS967. Peak current densities were not significantly different between control and GS967 conditions (control: 187.2 ± 32.6 pA/pF; GS967: 172.3 ± 46.2 pA/pF). (**C**) Representative spontaneous action potential firing recorded from a hippocampal pyramidal neuron from either wildtype (F1.WT) or *Scn2a*$^{Q54}$ (F1.Q54) mice. Membrane potential was clamped at −80 mV and spontaneous action potentials were recorded in the absence and presence of 1 µM GS967. (**D**) Concentration response of inhibition of spontaneous action potential firing by GS967 (closed circles) and inhibition action potential firing by 1 µM phenytoin (open square). Data are expressed as mean ± SEM, with n = 5-7 for each concentration (* $p < 0.05$) – Chris Thompson, PhD.

*Seizure frequency in Scn2a$^{Q54}$ mice is reduced by GS967*

We tested the ability of short-course (1-2 days) oral GS967 to reduce seizure frequency in *Scn2a*$^{Q54}$ mice. Mice maintained on 0.375 mg/kg/d GS967 exhibited a 50% reduction in seizure frequency whereas mice treated with higher dose (1.5 mg/kg/d) GS967 exhibited more than 90% seizure reduction following two days of treatment (Figure 3.6). The efficacy of this compound to suppress seizures in *Scn2a*$^{Q54}$ mice is similar to phenytoin (30 mg/kg), but the anticonvulsant effect of GS967 requires a much lower plasma concentration (Table 3.1). Vehicle controls for both GS967 and phenytoin treated animals exhibited no reduction in seizure frequency. It was observed that mice treated with phenytoin exhibited sedation characterized by lack of ambulation. Although there was a trend toward sedation, it was not significantly different from vehicle treated mice (5/7 awake for vehicle vs. 3/8 awake for phenytoin, $p = 0.31$). By contrast, no sedation was observed in GS967 and respective control treated animals.

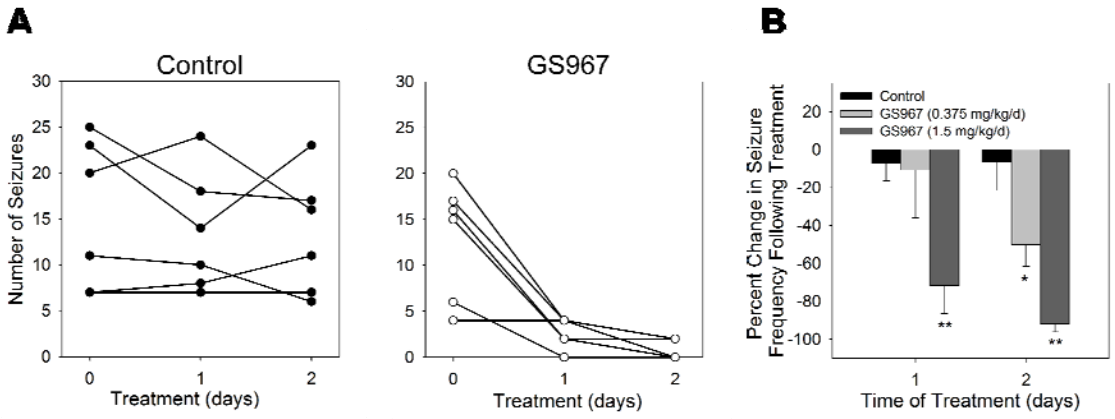


**Figure 3.6.** GS967 reduces seizure frequency in *Scn2a*$^{Q54}$ mice. (**A**) Number of seizures in 30 minutes for individual mice at baseline (day 0) and after treatment (day 1 and 2) with either control chow or 1.5 mg/kg/d GS967. (**B**) A histogram of percent change in seizure frequency following oral administration of either control or chow containing GS967 at two dosage levels. Percent change was calculated in response to treatment, with n = 6 for each treatment (*$p < 0.05$ and **$p < 0.005$ compared to control; repeated measures ANOVA).

*GS967 suppresses MES-induced seizures*

To further investigate the antiepileptic activity of GS967, we tested the ability of the compound to prevent MES-induced generalized tonic hindlimb seizures in wildtype C57BL/6J mice. Varying dosages of GS967 that yielded 0 to 100% protection were orally administered two hours prior to testing. Protection of MES-induced tonic hindlimb extension by GS967 was dose-dependent (Figure 3.7), with a calculated $ED_{50}$ value of 0.1 mg/kg. Vehicle treatment exhibited no protection against MES-induced seizures. For comparison, we experimentally determined an $ED_{50}$ value of ~5 mg/kg for phenytoin protection against MES-induced tonic hindlimb extension consistent with previously published data.[69] These observations indicate that GS967 has antiepileptic activity in two mechanistically divergent models of epilepsy.

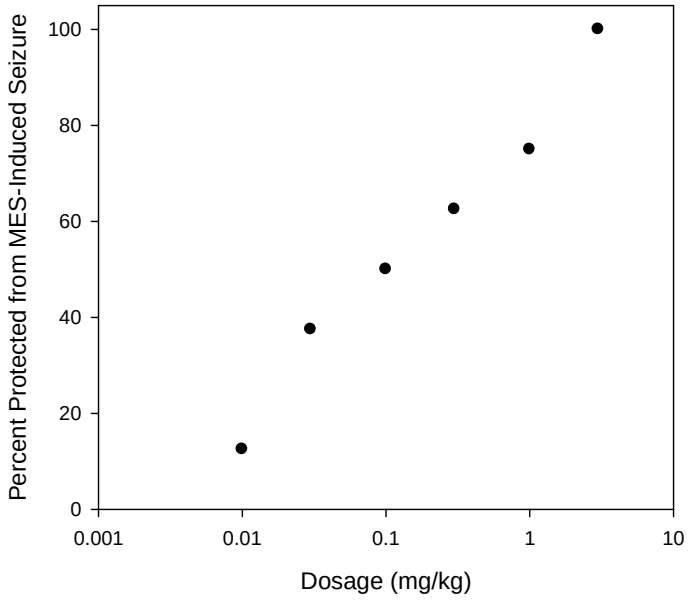


**Figure 3.7.** GS967 protects against MES-induced seizures. Dose response curve for seizure protection by GS967. Data are shown as percentage of animals protected from seizure at a given dose of drug, with n = 5-8 animals per dose. In collaboration with Wayne Frankel, PhD at The Jackson Laboratory.

*GS967 improves survival of Scn2a$^{Q54}$ mice*

*Scn2a*$^{Q54}$ mice have a significantly reduced lifespan with approximately 20% surviving to 12 weeks of age (Figure 3.8). Poor survival of *Scn2a*$^{Q54}$ mice has been attributed to chronic, unrelenting seizures with widespread neuronal injury. We tested whether preferential suppression of persistent current by GS967 would increase the lifespan of *Scn2a*$^{Q54}$ mice. Mice were continuously treated with GS967 beginning at postnatal day 21 and survival was monitored until 12 weeks of age. GS967 treatment dramatically improved the survival of *Scn2a*$^{Q54}$ mice with 90% of mice alive at 12 weeks compared to 20% survival of control (untreated) animals ($p < 0.005$; Figure 3.8).

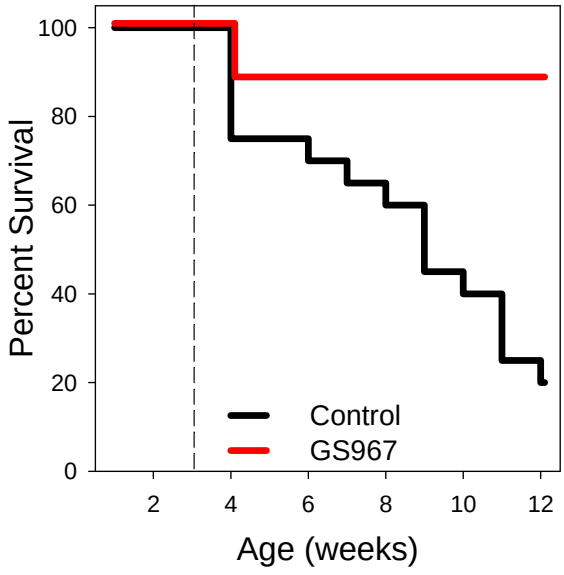


**Figure 3.8.** GS967 improves survival of *Scn2a*$^{Q54}$ mice. Survival curves of *Scn2a*$^{Q54}$ mice placed on control chow or chow containing GS967 (dose 1.5 mg/kg/d). Treatment began at 3 weeks of age indicated by the dashed line, with n = 18-20 per group. Survival difference between groups was significant at $p < 0.005$; Cox proportional hazards model.

*Survival of Scn1a$^{+/-}$ mice improved by GS967*

*Scn1a*$^{+/-}$ mice have a significantly reduced lifespan with only ~30% survival to 8 weeks of age (Figure 3.9). Poor survival of *Scn1a*$^{+/-}$ mice has been attributed to seizure clusters in a developmentally sensitive time window around the time of weaning. The seizures result from impaired GABA-mediated inhibition due to haploinsufficiency of *SCN1A*. We tested whether inhibition of persistent sodium current by GS967 would further impair GABA-mediated inhibition thereby exacerbating the phenotype of *Scn1a*$^{+/-}$ mice.

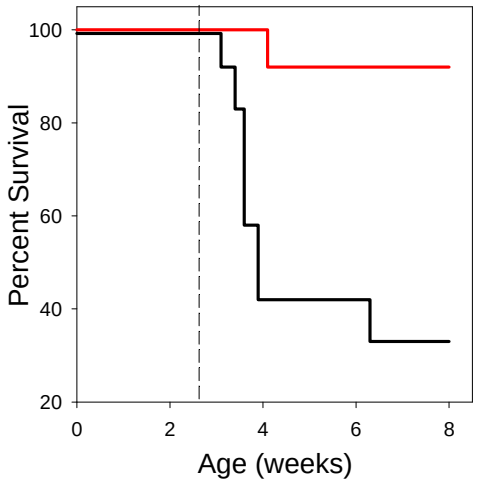


**Figure 3.9.** GS967 improves survival of *Scn1a*$^{+/-}$ mice. Survival curves of *Scn1a*$^{+/-}$ mice placed on control chow or chow containing GS967 (dose 1.5 mg/kg/d). Treatment began at 18 days of age indicated by the dashed line, with n = 12-13 per group. Survival difference between groups was significant at $p < 0.005$; Cox proportional hazards model.

*GS967 treatment prevents hilar neuron loss in Scn2a*$^{Q54}$ *mice*

Widespread neuronal loss in the dentate hilus is a commonly observed histopathological change in epilepsy patients and animal models of epilepsy, including the *Scn2a*$^{Q54}$ mouse model.[40,73,74] We investigated whether chronic GS967 treatment would prevent neuron loss in *Scn2a*$^{Q54}$ mice. Cresyl Violet staining revealed extensive neuronal cell loss in the

dentate hilus in 60 day-old *Scn2a*$^{Q54}$ mice compared to age-matched wildtype (WT) littermates (Figure 3.10) as reported previously.[40] By contrast, qualitatively, there was no overt hilar neuron loss in GS967 treated *Scn2a*$^{Q54}$ mice, indicating that GS967 treatment provides a neuronal preservation effect possibly by attenuating excitotoxicity caused by persistent sodium current.

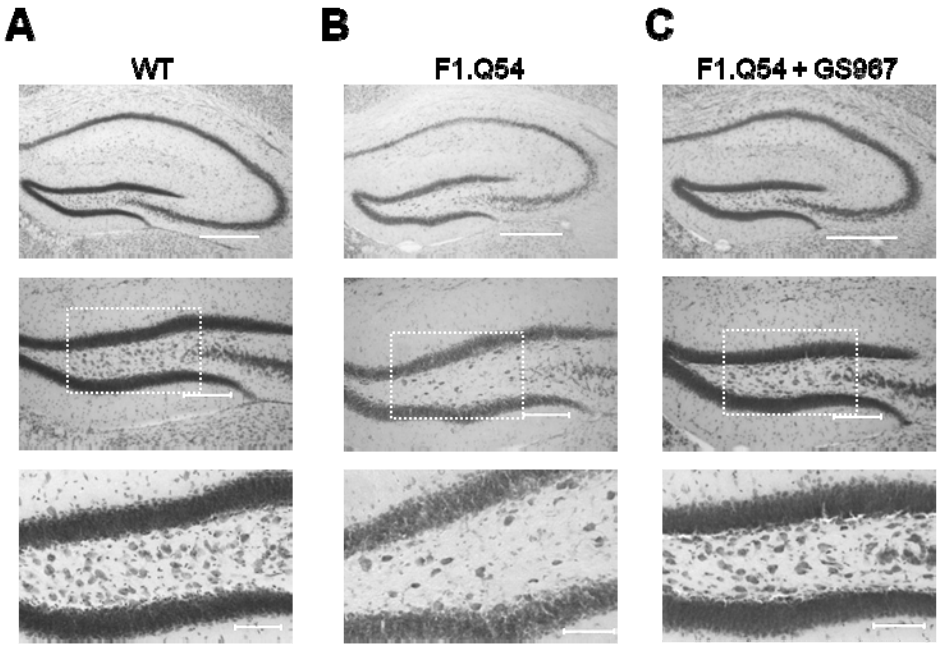


**Figure 3.10.** GS967 prevents hilar neuron loss in *Scn2a*$^{Q54}$ mice. **A**-**C**, Cresyl violet stained sections of the dentate gyrus from a representative wildtype mouse (WT, panel **A**), untreated *Scn2a*$^{Q54}$ mouse (F1.Q54, panel **B**) and a *Scn2a*$^{Q54}$ mouse treated with 1.5 mg/kg/d GS967 from age P21 to P60 (F1.Q54 + GS967, panel **C**). Images in the middle and lower panels are high-magnification views. Scale bars represent 500 μm, 200 μm and 100 μm for the upper, middle and lower panels, respectively.

*Mossy fiber sprouting is suppressed by GS967 treatment*

Seizure-induced sprouting of the mossy fiber pathway in the dentate gyrus is a frequently observed morphological change associated with epilepsy and has also been observed in *Scn2a*$^{Q54}$ mice.[40,74] We tested whether chronic GS967 treatment of *Scn2a*$^{Q54}$ mice would

attenuate mossy fiber sprouting. Using Timm staining, we observed evidence of robust mossy fiber sprouting within the inner molecular layer of the dentate gyrus in 60 day-old *Scn2a*$^{Q54}$ mice compared to age-matched WT littermates (Figure 3.11 A,B). By contrast, *Scn2a*$^{Q54}$ mice chronically treated with GS967 exhibited a low density of Timm staining (Figure 3.11). Mossy fiber sprouting was quantified in the inner molecular layer of the dentate gyrus using densitometry normalized to background staining. There was a significant ($p < 0.05$) reduction in the extent of mossy fiber sprouting in GS967 treated *Scn2a*$^{Q54}$ mice (1.32 ± 0.12) compared to untreated *Scn2a*$^{Q54}$ (1.81 ± 0.16*) and WT (1.36 ± 0.07) animals. These findings indicate that chronic seizure suppression by GS967 suppressed mossy fiber sprouting in *Scn2a*$^{Q54}$ mice.

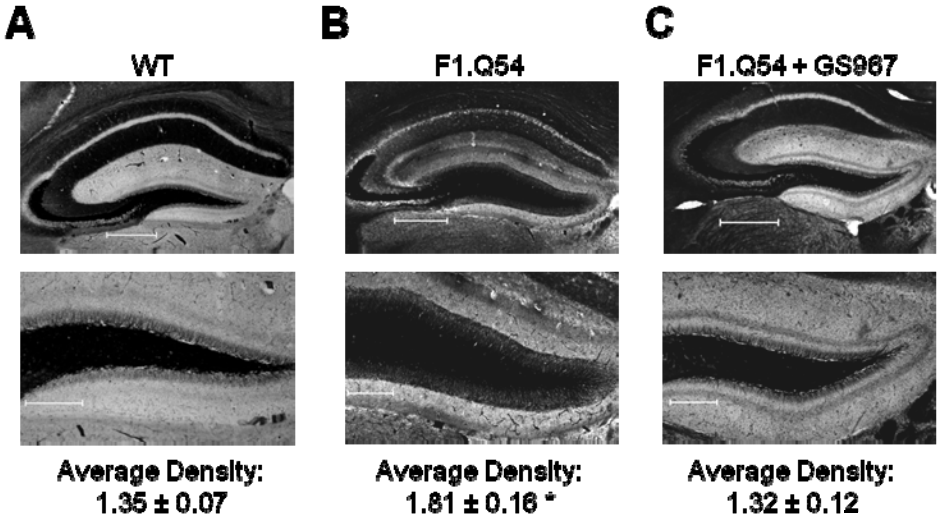


**Figure 3.11.** GS967 suppresses mossy fiber sprouting in *Scn2a*$^{Q54}$ mice. **A**-**C**, Timm stained sections of the dentate gyrus from a wildtype (WT, panel **A**) untreated *Scn2a*$^{Q54}$ mouse (F1.Q54, panel **B**) and a *Scn2a*$^{Q54}$ mouse treated with GS967 from age P21 to P60 (F1.Q54 + GS967, panel **C**). Images in the lower panels are high-magnification views. Scale bars represent 500 μm and 200 μm for the upper and lower panels, respectively. Quantification of the average density in the inner molecular layer of the dentate gyrus normalized to background is reported below images. Data are expressed as mean ± SEM, with n = 6-8 per group (*$p < 0.05$; one-way ANOVA followed by Tukey HSD post-hoc).

## DISCUSSION

In this study, we determined the anticonvulsant effect of ranolazine and GS967, two persistent sodium current blockers. AEDs targeting voltage-gated sodium channels have existed for many years, and most exert their clinical effects through use-dependent block of transient sodium current in a manner similar to that of local anesthetics. Use-dependent block of the transient sodium current can dampen neuronal excitability especially during rapid firing such as the hypersynchronous bursts associated with seizures. While some AEDs may also suppress persistent sodium current to some extent, no currently approved AED has a strong preference blocking this activity.[75]

### *Persistent sodium current and epilepsy*

Under normal physiological conditions, opening of voltage-gated sodium channels is short-lived and lasts only a few milliseconds before the process of fast inactivation returns current levels to near baseline values. However, a small amount of sodium current may persist after the main transient current is extinguished. This persistent sodium current can influence neuronal firing by amplifying subthreshold synaptic inputs or evoking a sustained membrane depolarization.[59] The ability of persistent sodium current to promote neuronal excitability has led to speculation that this current may contribute to epilepsy possibly by allowing pathological firing frequencies or by enabling the spread of epileptic neuronal activity.

Several lines of evidence support the hypothesis that persistent sodium current can be epileptogenic. Mutations in human $Na_V1.1$, $Na_V1.2$, $Na_V1.3$ and $Na_V1.6$ sodium channels

have been associated with a spectrum of genetic epilepsies. *In vitro* experiments probing the functional consequences of several human mutations have revealed increased persistent sodium current as a major, and sometimes solitary, defect.[26,66,76-79] Further, low level expression of a mutant $Na_V1.2$ transgene exhibiting increased persistent current in the *Scn2a*$^{Q54}$ mouse model demonstrates the pathogenic nature of this current.[40] Additionally, Chen and colleagues demonstrated high-threshold bursting in hippocampal CA1 neurons is driven by persistent sodium current in the pilocarpine-induced status epilepticus rat model of temporal lobe epilepsy.[80] The authors speculate that increased persistent sodium current contributes to establishing chronic epilepsy in this rodent model. More recently, evidence from *Drosophila* demonstrate important contributions of persistent neuronal sodium current to seizure phenotypes arising from spontaneous and engineered mutants.[81,82] While increased persistent current does not account for all genetic epilepsies arising from mutant sodium channels, this mechanism appears to be an important contributor in many situations.

*Anticonvulsant activity of GS967*

GS967 has previously been shown to preferentially inhibit persistent sodium current mediated by the cardiac voltage gated sodium channel and is an effective suppressor of ventricular arrhythmias.[63,64] Unlike ranolazine, GS967 is capable of effectively penetrating the blood brain barrier and has slow elimination from the body, suggesting that this compound may have more efficacious antiepileptic activity. Our data show that GS967 was capable of preferentially suppressing persistent sodium current mediated by a neuronal voltage-gated sodium channel with greater potency than the commonly

prescribed AED phenytoin, and inhibited spontaneous action potentials in pyramidal neurons isolated from *Scn2a*$^{Q54}$ mice. Importantly, GS967 suppressed seizures in both the MES-induced seizure model and the *Scn2a*$^{Q54}$ mouse model of epilepsy.

Many Dravet syndrome patients treated with sodium channel blockers such as lamotrigine show no benefit, and in some cases, experience worsening epilepsy.[58] Therefore, we hypothesized that because GS967 selectively inhibits voltage-gated sodium channels, *Scn1a*$^{+/-}$ mice would be refractory to GS967 treatment. Surprisingly, however, GS967 treatment significantly improved the lifespan of *Scn1a*$^{+/-}$ mice. Initial studies suggested that Dravet syndrome stemmed from a loss of GABAergic inhibitory tone. However, more recent studies have shown that in addition to impaired GABA-mediated inhibition, the mechanism responsible for Dravet syndrome may also involve a hyperexcitable component resulting from hyperactive pyramidal neurons. Specifically, pyramidal neurons isolated from *Scn1a*$^{+/-}$ mice showed an increased sodium current density and a hyperpolarizing shift in the voltage-dependence of activation compared to wildtype animals which is consistent with hyperexcitability.[44] Additionally, differentiated pyramidal neurons derived from Dravet syndrome patient iPSCs exhibit increased sodium current density and hyperexcitability.[55] We propose that GS967 prolongs the lifespan of *Scn1a*$^{+/-}$ mice by inhibiting the abnormal voltage-gated sodium current observed in hippocampal pyramidal neurons, thereby reducing overall excitability.

*GS967 suppresses mossy fiber sprouting*

Mossy fiber sprouting refers to the aberrant growth of granule cell axons (mossy fibers) into the inner molecular layer of the dentate gyrus.[74] This phenomenon has been observed in patients with epileptic seizures and in animal models of epilepsy, but the contribution of mossy fiber sprouting to epileptogenesis remains unclear and controversial. Substantial evidence supports the idea that the sprouted fibers form synapses on granule cells and generate recurrent excitatory circuits capable of perpetuating seizure activity.[74] Attempts to inhibit mossy fiber sprouting using commonly prescribed AEDs, including the voltage-gated sodium channel inhibitor lamotrigine, have been largely unsuccessful.[83-86] Inhibition of the mammalian target of rapamycin (mTOR) signaling pathway has been demonstrated to suppress mossy fiber sprouting in animal models of temporal lobe epilepsy.[87] Our results appear to represent the first example of a sodium channel blocking drug with anticonvulsant properties capable of suppressing mossy fiber sprouting in an epileptic animal model.

## CONCLUSION

We demonstrated anticonvulsant activity for two preferential persistent sodium current blockers. We further demonstrated that GS967 is a potent and selective inhibitor of persistent current that suppresses seizure activity in two mouse models, dampens hippocampal neuronal excitability in a concentration-dependent manner, prolongs survival of genetic epilepsy models, and prevents both hilar neuron loss and development of mossy fiber sprouting in these mice. Our findings provide evidence suggesting that

preferential inhibition of persistent sodium current is an effective strategy for development of new AEDs.

# CHAPTER IV

## PERSPECTIVES AND FUTURE DIRECTIONS

*Summary*

Epilepsy is one of the most common neurological disorders affecting approximately 50 million people of all ages worldwide.[88] Nearly two-thirds of patients diagnosed with epilepsy develop seizures with no obvious brain lesions or any other neurological abnormalities, so are presumed to be of genetic origin.[1] These genetic epilepsies exhibit complex inheritance suggesting the involvement of multiple genes and environmental factors. Recent studies, however, have identified monogenic epilepsies in which the syndromes arise from mutations within single genes. All of the identified mutations occur in genes essential for neuronal signaling such as nicotinic acetylcholine receptors, $GABA_A$ receptors and voltage-gated ion channels, with mutations within voltage-gated sodium channels the most prevalent.[17,24] Information gained from the identification and characterization of these mutant alleles has provided insight into the molecular mechanisms that underlie the pathology of epilepsy and have inspired the development of new therapies.

The need for novel therapeutics is highlighted by the fact that 30% of epilepsy patients do not achieve seizure control with currently available AEDs, which creates a great burden both physically and socially.[8] Drug resistant epilepsy represents an unmet medical challenge in the field that needs to be addressed and new therapies need to be developed.

*Animal models of epilepsy*

While animal models have been extensively used in the past for the development and testing of AEDs, they may not accurately depict human epilepsy. A definite limitation of these models is that they are induced seizure models rather than epilepsy models.[8] Animal models that exhibit spontaneous seizures are more etiologically relevant for investigating the neurophysiological basis of epilepsy and for testing new AEDs. The availability of two genetic mouse models of epilepsy have provided a platform to study molecular mechanisms of epileptogenesis as well as a new testing ground for evaluating novel therapeutic strategies. One drug that has come from such studies is GS967. The compound GS967 is a potent and selective inhibitor of persistent sodium current which is a biophysical defect observed in association with some genetic epilepsies. We tested the antiepileptic potential of GS967 and found that this compound was effective across multiple mouse models of epilepsy representing both gain- and loss-of-function phenotypes.

*Effectiveness of GS967 in multiple mouse models of epilepsy*

The *Scn2a*$^{Q54}$ genetically engineered mouse model of mesial temporal lobe epilepsy expresses a transgene encoding a gain-of-function $Na_v1.2$ channel. *Scn2a*$^{Q54}$ mice exhibit spontaneous seizures and premature death hypothesized to result from increased persistent sodium current in hippocampal neurons.[40] We utilized the *Scn2a*$^{Q54}$ mouse model of epilepsy to test the hypothesis that preferential inhibition of persistent sodium current would represent a novel antiepileptic drug mechanism. We showed that GS967

reduced seizure frequency and improved survival of *Scn2a*$^{Q54}$ mice. These results indicate that GS967 is an effective AED in this genetic mouse model of epilepsy. Phenytoin, a conventional AED, also reduced seizure frequency in *Scn2a*$^{Q54}$ mice, which validates the *Scn2a*$^{Q54}$ model as a relevant model for testing new AEDs. The *Scn2a*$^{Q54}$ mouse model represents a genetic model with spontaneous, recurrent seizures that could prove to be instrumental for evaluating novel compounds during AED development, particularly those with a target-based design strategy.

We also found that GS967 was effective in the heterozygous *Scn1a* knockout (*Scn1a*$^{+/-}$) mouse model of epilepsy. Heterozygous deletion of *Scn1a* in mice models Dravet syndrome in human epilepsy. *Scn1a*$^{+/-}$ mice exhibit severe, spontaneous seizures and premature death. They also display a reduced threshold to induced seizures (flurothyl and hyperthermia) and cognitive and motor impairments.[42-44] *Scn1a*$^{+/-}$ mice are excellent models of spontaneous genetic epilepsy that can be used to investigate mechanisms of epileptogenesis and exploited for AED development. Long-term GS967 treatment dramatically improved the survival of *Scn1a*$^{+/-}$ mice, a result that was unanticipated. Initial work in *Scn1a*$^{+/-}$ mice showed reduced sodium current density and excitability in GABAergic interneurons leading to the interneuron-hypothesis of Dravet syndrome, which postulates that the loss of GABA-mediated inhibition is the underlying physiological mechanism of epileptogenesis. We had hypothesized that GS967 would exacerbate the phenotype of *Scn1a*$^{+/-}$ mice because GS967 would further inhibit *Scn1a* which already exhibits haploinsufficiency. Because GS967 was effective in *Scn1a*$^{+/-}$ mice, it suggests a more complex pathophysiology than was originally hypothesized.

This is consistent with recent work showing that excitatory pyramidal neuron dysfunction may contribute to the pathophysiology of Dravet syndrome. Increased sodium current density and excitability of pyramidal neurons was recorded in both *Scn1a*$^{+/-}$ mice and Dravet syndrome derived iPSCs.[44,55] These results postulate that Dravet syndrome may reflect a combination of abnormalities within interneurons and pyramidal neurons that create a significant imbalance in excitatory and inhibitory neurotransmission and promote network hyperexcitability. Interestingly, withdrawal of GS967 at 9 weeks from a cohort of mice showed long-term effects as survival was maintained to 12 weeks of age. The benefits of GS967 in *Scn1a*$^{+/-}$ mice that persist in the absence of drug suggest that there is a critical period of vulnerability in which *Scn1a*$^{+/-}$ mice are extremely susceptible to premature death and treatment through this period yields long-term survival.

GS967 represents a novel pharmacological tool that could prove beneficial for investigating the neurophysiological mechanisms responsible for epileptogenesis in Dravet syndrome. Additionally, GS967 may have potential as a therapeutic for Dravet syndrome patients. We have shown that GS967 improves the lifespan of *Scn1a*$^{+/-}$ mice. The question that still remains, however, is whether GS967 can rescue the seizure phenotype of *Scn1a*$^{+/-}$ mice. *Scn1a*$^{+/-}$ mice exhibit spontaneous seizure and reduced thresholds for flurothyl- and hyperthermia-induced seizures when compared to wildtype animals. Future experiments should monitor the occurrence of spontaneous seizures and evaluate seizure thresholds following GS967 treatment. Electrophysiological experiments in hippocampal slices in the presence of GS967 would provide further insight into the

pathogenesis of Dravet syndrome which can be used to inform the development of novel therapeutics.

*GS967 as a novel antiepileptic drug*

The effectiveness of GS967 as an antiepileptic drug was confirmed in three mechanistically distinct mouse models of epilepsy. GS967 reduced seizure frequency and prolonged the lifespan of *Scn2a*$^{Q54}$ mice. GS967 also protected against induced seizures in the maximal electroshock (MES) seizure model. Phenytoin was used as a comparator in the *Scn2a*$^{Q54}$ and MES models and in both cases GS967 was more potent at seizure suppression. No adverse consequences were observed with GS967 treatment. Additionally, GS967 prevented hilar neuron loss and suppressed mossy fiber sprouting in *Scn2a*$^{Q54}$ mice which appears to be the first example of a sodium channel blocking drug with antiepileptic properties capable of preventing mossy fiber sprouting, an added benefit of GS967 as an AED. *Scn1a*$^{+/-}$ mice which model the drug refractory epileptic encephalopathy, Dravet syndrome, benefited from GS967 treatment. GS967 treatment improved the lifespan of *Scn1a*$^{+/-}$ mice further promoting its utility as an effective AED. GS967 has a large therapeutic window and is selective for voltage-gated sodium channels as it does not affect other ion channels, transporters, receptors or kinases. The safety profile of GS967 coupled with its success in multiple mouse models of epilepsy certainly warrants consideration for a New Drug Application to move studies into higher organisms with the eventual goal of GS967 as a viable treatment option for epilepsy patients.

*Gad67-SCN1A genetic rescue of Scn1a$^{+/-}$ mice*

Studies in *Scn1a*$^{+/-}$ mice have provided the field with many clues regarding the cellular and molecular mechanisms that contribute to the pathology of Dravet syndrome. We have used the *Scn1a*$^{+/-}$ mouse model to further probe the pathophysiology of Dravet syndrome and to investigate potential therapies to rescue the epilepsy phenotype. As described previously, we found that GS967 has AED properties in *Scn1a*$^{+/-}$ mice. Results from those experiments and recent work in pyramidal neurons are suggestive of a more complex pathophysiological mechanism than was initially hypothesized. The idea of a combination pathology for Dravet syndrome, including interneuron and pyramidal neuron abnormalities, is further supported by observations made in the *Gad67-SCN1A* transgenic rescue experiments. We generated three independent *Gad67-SCN1A* transgenic mouse lines selectively expressing *SCN1A* in GABAergic rneurons and attempted to rescue the Dravet syndrome phenotype of *Scn1a*$^{+/-}$ mice. We hypothesized that if Dravet syndrome exhibits an interneuron-specific pathology, then restoration of *SCN1A* selectively in inhibitory neurons of *Scn1a*$^{+/-}$ mice would rescue the epilepsy phenotype. The *Gad67-SCN1A* genetic approach that we utilized was not sufficient to attenuate or prevent the phenotype of *Scn1a*$^{+/-}$ mice. Additional experiments need to be performed to further characterize the three *Gad67-SCN1A* transgenic lines and will provide insight into why restoration of *SCN1A* did not alleviate the phenotype. We need to conduct experiments to determine the transgene integration site into the genome to ensure that our results are not confounded by the fact that the transgene disrupted expression of an essential gene. We also need to confirm the *SCN1A* is localized to GABAergic neurons. Western blot analysis shows varying levels of *SCN1A* transgene across the *Gad67-SCN1A* lines.

Future electrophysiological experiments will determine the interneuron sodium current density associated with each transgenic line and compare to endogenous wildtype levels. These experiments will inform us whether there is inadequate or excess sodium current restored. It is also plausible that the epilepsy phenoptype was not rescued by the *Gad67-SCN1A* transgenic strategy because the interneuron only explanation for Dravet syndrome is an overly simplified model, and in fact other neuronal populations may also contribute to the disease.

*Lamotrigine and Scn1a*$^{+/-}$ :: *SCN1A*$^{RC/+}$ *mice*

We also generated two independent *Gad67-SCN1A-R1648C* transgenic mouse lines which express mutant *SCN1A* selectively in GABAergic neurons. The *SCN1A* mutation R1648C has been identified in association with Dravet syndrome.[29] Previous studies of *SCN1A-R1648C* demonstrated impaired cell surface trafficking, reduced sodium current density and increased persistent sodium current compared to wildtype channels.[35,89] Treatment of cells expressing *SCN1A-R1648C* with the conventional sodium channel inhibitors, lamotrigine and phenytoin, has shown increased cell surface expression.[35] A paradoxical phenomenon in the treatment of Dravet syndrome is that clinically, some patients experience worsening seizures in response to treatment with sodium channel blockers such as lamotrigine.[58] There are no models in which AED-induced exacerbation of epilepsy has been modeled and the current Dravet syndrome models do not really offer any explanations either. The *Gad67-SCN1A-R1648C* transgenic lines provide a unique opportunity to examine potential mechanisms underlying exacerbation of Dravet syndrome by certain AEDs. We will use the mutant transgenic mice to test the

hypothesis that lamotrigine treatment exaggerates the phenotype of Dravet syndrome by increasing cell surface expression of a dysfunctional channel. Future experiments will need to evaluate the seizure phenotype of combined knockout/transgenic mice (*Scn1a*$^{+/-}$ :: *SCN1A*$^{RC/+}$) following chronic lamotrigine treatment. Additionally, *in vivo* experiments examining the effect of lamotrigine treatment on cell surface expression of *SCN1A-R1648C* need to be conducted. Results from these experiments could provide a mechanistic basis for the adverse effects of some treatment strategies in Dravet syndrome. Furthermore, *Scn1a*$^{+/-}$ :: *SCN1A*$^{RC/+}$ mice would provide an actual model of spontaneous, drug-resistant epilepsy.

*Conclusions*

Historically, animals have been used for evaluating the safety of compounds intended for human use. Advances in medical science and genetic manipulations have led to the generation of animal models of human diseases that have provided groundbreaking insight into the cellular and molecular mechanisms underlying the pathology of disease. Additionally, animal models have been invaluable inspiration for directing the development and for testing the efficacy of novel therapeutics. The field of epilepsy is not excluded from the benefits surrounding the use of animal models. Simple seizure models have been used for decades to screen compounds for AED discovery and identify potential drug candidates. A disadvantage of these simple seizure models is that they model acute seizures rather than genetic epilepsy. Genetic engineering, however, has enabled the generation of mouse models of epilepsy that are more etiologically relevant to human epilepsy. Two distinct models have been described exhaustively throughout

this thesis. The transgenic *Scn2a*$^{Q54}$ mouse model of mesial temporal lobe epilepsy expresses a gain-of-function mutation in a neuronal $Na_v1.2$ channel and exhibits spontaneous seizures. While the *Scn2a*$^{Q54}$ mouse model has been used extensively in the past to investigate mechanisms of epileptogenesis, we used the *Scn2a*$^{Q54}$ model for AED development to test a hypothesis-driven, target-based treatment strategy. We discovered that preferential persistent sodium current inhibition is an effective AED mechanism and GS967 was identified as a potent AED. Since *Scn2a*$^{Q54}$ mice are a model of epilepsy, it should be considered as a primary model of epilepsy to be used in future AED development. The second genetic model that exhibits epilepsy is the *Scn1a*$^{+/-}$ mouse model, which mirrors Dravet syndrome. The *Scn1a*$^{+/-}$ mouse model has primarily been used to investigate the disease mechanism of Dravet syndrome, with the goal being that once the pathophysiological mechanism is understood it can be converted to develop therapeutic strategies. The common hypothesis responsible for the pathology of Dravet syndrome involves a loss of GABA-mediated inhibition due to haploinsufficiency of *SCN1A*. Although experiments are still ongoing, we are using *Scn1a*$^{+/-}$ mice to further investigate the molecular basis for Dravet syndrome by utilizing a genetic approach to rescue the phenotype. Results from these experiments could be used to inform development of target-based strategies in the treatment of Dravet syndrome. Serendipitously, we found that GS967 has a beneficial effect in *Scn1a*$^{+/-}$ mice, a result that could translate into an effective treatment strategy for Dravet syndrome. *Scn1a*$^{+/-}$ mice model epilepsy and should also be used in the development of novel AEDs.

Through the use of animal models of epilepsy, we were able to identify a novel compound, GS967, that shows great potential as an antiepileptic drug. GS967 was

effective in three mechanistically different mouse models of epilepsy, making it a promising candidate for human epilepsy patients.

REFERENCES


1. Hauser, W. A., Annegers, J. F. & Kurland, L. T. Incidence of epilepsy and unprovoked seizures in Rochester, Minnesota: 1935-1984. *Epilepsia* **34**, 453-468 (1993).

2. Leonardi, M. & Ustun, T. B. The global burden of epilepsy. *Epilepsia* **43 Suppl 6**, 21-25 (2002).

3. Sander, J. W. The epidemiology of epilepsy revisited. *Curr. Opin. Neurol.* **16**, 165-170 (2003).

4. Goodman & Gilman *Goodman and Gilman's The Pharmacological Basis of Therapeutics*. (2006).

5. Hui, Y. Y., Ahmad, N. & Makmor-Bakry, M. Pathogenesis of Epilepsy: Challenges in Animal Models. *Iran J. Basic Med. Sci.* **16**, 1119-1132 (2013).

6. Berg, A. T. *et al.* Revised terminology and concepts for organization of seizures and epilepsies: report of the ILAE Commission on Classification and Terminology, 2005-2009. *Epilepsia* **51**, 676-685 (2010).

7. Ghaffarpour, M. *et al.* Pharmacokinetic and pharmacodynamic properties of the new AEDs: A review article. *Iran J. Neurol.* **12**, 157-165 (2013).

8. Loscher, W., Klitgaard, H., Twyman, R. E. & Schmidt, D. New avenues for anti-epileptic drug discovery and development. *Nat. Rev. Drug Discov.* **12**, 757-776 (2013).

9. Putnam, T. J. & Merritt, H. H. Experimental determination of the anticonvulsant properties of some phenyl derivatives. *Science* **85**, 525-526 (1937).

10. Swinyard, E. A., Brown, W. C. & Goodman, L. S. Comparative assays of antiepileptic drugs in mice and rats. *J. Pharmacol. Exp. Ther.* **106**, 319-330 (1952).

11. Goddard, G. V., McIntyre, D. C. & Leech, C. K. A permanent change in brain function resulting from daily electrical stimulation. *Exp. Neurol.* **25**, 295-330 (1969).

12. Everett, G. M. & Richards, R. K. Comparative anticonvulsive action of 3,5,5-trimethyloxazolidine-2,4,dione (tridione), dilantin and phenobarbitol. *J Phramacol* **81**, 402-407 (1944).

13. Ben-Ari, Y., Tremblay, E., Ottersen, O. P. & Naquet, R. Evidence suggesting secondary epileptogenic lesion after kainic acid: pre treatment with diazepam reduces distant but not local brain damage. *Brain Res.* **165**, 362-365 (1979).

14. Cavalheiro, E. A. *et al.* Long-term effects of pilocarpine in rats: structural damage of the brain triggers kindling and spontaneous recurrent seizures. *Epilepsia* **32**, 778-782 (1991).

15. Marescaux, C., Vergnes, M. & Depaulis, A. Genetic absence epilepsy in rats from Strasbourg--a review. *J. Neural Transm. Suppl* **35**, 37-69 (1992).

16. Barton, M. E., Klein, B. D., Wolf, H. H. & White, H. S. Pharmacological characterization of the 6 Hz psychomotor seizure model of partial epilepsy. *Epilepsy Res.* **47**, 217-227 (2001).

17. Meisler, M. H., Kearney, J., Ottman, R. & Escayg, A. Identification of epilepsy genes in human and mouse. *Annu. Rev. Genet* **35**, 567-588 (2001).

18. Catterall, W. A. Cellular and molecular biology of voltage-gated sodium channels. *Physiologic Rev* **72**, S15-S48 (1992).

19. Catterall, W. A. From ionic currents to molecular mechanisms: the structure and function of voltage-gated sodium channels. *Neuron* **26**, 13-25 (2000).

20. George, A. L., Jr. Inherited disorders of voltage-gated sodium channels. *J Clin Invest* **115**, 1990-1999 (2005).

21. Meisler, M. H. & Kearney, J. A. Sodium channel mutations in epilepsy and other neurological disorders. *J Clin Invest* **115**, 2010-2017 (2005).

22. Vacher, H., Mohapatra, D. P. & Trimmer, J. S. Localization and targeting of voltage-dependent ion channels in mammalian central neurons. *Physiologic Rev* **88**, 1407-1447 (2008).

23. Parihar, R. & Ganesh, S. The SCN1A gene variants and epileptic encephalopathies. *J. Hum. Genet.* **58**, 573-580 (2013).

24. Catterall, W. A. Sodium Channel Mutations and Epilepsy. (2012).

25. Spampanato, J., Escayg, A., Meisler, M. H. & Goldin, A. L. Generalized epilepsy with febrile seizures plus type 2 mutation W1204R alters voltage-dependent gating of $Na_{V1.1\ sodium\ channels}$. *Neuroscience* **116**, 37-48 (2003).

26. Lossin, C., Wang, D. W., Rhodes, T. H., Vanoye, C. G. & George, A. L., Jr. Molecular basis of an inherited epilepsy. *Neuron* **34**, 877-884 (2002).

27. Escayg, A. *et al.* A novel *SCN1A* mutation associated with generalized epilepsy with febrile seizures plus - and prevalence of variants in patients with epilepsy. *Am J Hum Genet* **68**, 866-873 (2001).

28. Spampanato, J. *et al.* A novel epilepsy mutation in the sodium channel SCN1A identifies a cytoplasmic domain for beta subunit interaction. *J Neurosci* **24**, 10022-10034 (2004).

29. Escayg, A. *et al.* Mutations of SCN1A, encoding a neuronal sodium channel, in two families with GEFS+2. *Nature Genet* **24**, 343-345 (2000).

30. Cossette, P. *et al.* Functional characterization of the D188V mutation in neuronal voltage-gated sodium channel causing generalized epilepsy with febrile seizures plus (GEFS). *Epilepsy Res.* **53**, 107-117 (2003).

31. Rhodes, T. H., Lossin, C., Vanoye, C. G., Wang, D. W. & George, A. L., Jr. Noninactivating voltage-gated sodium channels in severe myoclonic epilepsy of infancy. *Proc Natl Acad Sci U S A* **101**, 11147-11152 (2004).

32. Wallace, R. H. *et al.* Febrile seizures and generalized epilepsy associated with a mutation in the $Na^+$-channel β1 subunit gene *SCN1B*. *Nature Genet* **19**, 366-370 (1998).

33. Spampanato, J., Escayg, A., Meisler, M. H. & Goldin, A. L. Functional effects of two voltage-gated sodium channel mutations that cause generalized epilepsy with febrile seizures plus type 2. *J Neurosci* **21**, 7481-7490 (2001).

34. Lossin, C. *et al.* Epilepsy-associated dysfunction in the voltage-gated neuronal sodium channel SCN1A. *J Neurosci* **23**, 11289-11295 (2003).

35. Thompson, C. H., Porter, J. C., Kahlig, K. M., Daniels, M. A. & George, A. L., Jr. Nontruncating SCN1A mutations associated with severe myoclonic epilepsy of infancy impair cell surface expression. *J. Biol. Chem.* **287**, 42001-42008 (2012).

36. Sugawara, T. *et al.* $Na_V1.1$ channels with mutations of severe myoclonic epilepsy in infancy display attenuated currents. *Epilepsy Research* **54**, 201-207 (2003).

37. Claes, L. *et al.* De novo mutations in the sodium-channel gene SCN1A cause severe myoclonic epilepsy of infancy. *Am J Hum Genet* **68**, 1327-1332 (2001).

38. Ohmori, I., Ouchida, M., Ohtsuka, Y., Oka, E. & Shimizu, K. Significant correlation of the SCN1A mutations and severe myoclonic epilepsy in infancy. *Biochem. Biophys. Res. Commun.* **295**, 17-23 (2002).

39. Ogiwara, I. *et al.* $Na_V1.1$ localizes to axons of parvalbumin-positive inhibitory interneurons: a circuit basis for epileptic seizures in mice carrying an *Scn1a* gene mutation. *J Neurosci.* **27**, 5903-5914 (2007).

40. Kearney, J. A. *et al.* A gain-of-function mutation in the sodium channel gene Scn2a results in seizures and behavioral abnormalities. *Neuroscience* **102**, 307-317 (2001).

41. Bergren, S. K., Chen, S., Galecki, A. & Kearney, J. A. Genetic modifiers affecting severity of epilepsy caused by mutation of sodium channel Scn2a. *Mamm. Genome.* **16**, 683-690 (2005).

42. Yu, F. H. *et al.* Reduced sodium current in GABAergic interneurons in a mouse model of severe myoclonic epilepsy in infancy. *Nature Neurosci* **9**, 1142-1149 (2006).

43. Miller, A. R., Hawkins, N. A., McCollom, C. E. & Kearney, J. A. Mapping genetic modifiers of survival in a mouse model of Dravet syndrome. *Genes Brain Behav.* **13**, 163-172 (2014).

44. Mistry, A. M. *et al.* Strain- and age-dependent hippocampal neuron sodium currents correlate with epilepsy severity in Dravet syndrome mice. *Neurobiol. Dis.* **65C**, 1-11 (2014).

45. Engel, J., Jr. Intractable epilepsy: definition and neurobiology. *Epilepsia* **42 Suppl 6**, 3 (2001).

46. Dravet, C., Bureau, M., Guerrini, R., Giraud, N. & Toger, J. *Epileptic Syndromes in Infancy, Childhood and Adolescence*. Rogers, J., Bureau, M., Dravet, C., Dreifuss, F. E. & Wolf, P. (eds.), pp. 75-88 (John Libbey, London,1992).

47. Oguni, H., Hayashi, K., Awaya, Y., Fukuyama, Y. & Osawa, M. Severe myoclonic epilepsy in infants--a review based on the Tokyo Women's Medical University series of 84 cases. *Brain Dev.* **23**, 736-748 (2001).

48. Claes, L. R. *et al.* The SCN1A variant database: a novel research and diagnostic tool. *Hum. Mutat.* (2009).

49. Lossin, C. A catalog of SCN1A variants. *Brain Dev.* **31**, 114-130 (2009).

50. Cheah, C. S. *et al.* Specific deletion of NaV1.1 sodium channels in inhibitory interneurons causes seizures and premature death in a mouse model of Dravet syndrome. *Proc. Natl. Acad. Sci. U. S. A* **109**, 14646-14651 (2012).

51. Hartshorne, R. P. & Catterall, W. A. Purification of the saxitoxin receptor of the sodium channel from rat brain. *Proc. Natl. Acad. Sci. U. S. A* **78**, 4620-4624 (1981).

52. Hawkins, N. A., Martin, M. S., Frankel, W. N., Kearney, J. A. & Escayg, A. Neuronal voltage-gated ion channels are genetic modifiers of generalized epilepsy with febrile seizures plus. *Neurobiol. Dis.* **41**, 655-660 (2011).

53. Oliva, A. A., Jr., Jiang, M., Lam, T., Smith, K. L. & Swann, J. W. Novel hippocampal interneuronal subtypes identified using transgenic mice that express green fluorescent protein in GABAergic interneurons. *J Neurosci.* **20**, 3354-3368 (2000).

54. Wilson, M. H., Coates, C. J. & George, A. L., Jr. PiggyBac Transposon-mediated Gene Transfer in Human Cells. *Mol. Ther.* **15**, 139-145 (2007).

55. Liu, Y. *et al.* Dravet syndrome patient-derived neurons suggest a novel epilepsy mechanism. *Ann. Neurol.* **74**, 128-139 (2013).

56. McBain, C. J. & Fisahn, A. Interneurons unbound. *Nat. Rev. Neurosci.* **2**, 11-23 (2001).

57. Kepecs, A. & Fishell, G. Interneuron cell types are fit to function. *Nature* **505**, 318-326 (2014).

58. Guerrini, R. *et al.* Lamotrigine and seizure aggravation in severe myoclonic epilepsy. *Epilepsia* **39**, 508-512 (1998).

59. Stafstrom, C. E. Persistent sodium current and its role in epilepsy. *Epilepsy Curr.* **7**, 15-22 (2007).

60. George, A. L. J. Inherited disorders of voltage-gated sodium channels. *J. Clin. Invest.* **115**, 1990-1999 (2005).

61. Kahlig, K. M., Lepist, I., Leung, K., Rajamani, S. & George, A. L. Ranolazine selectively blocks persistent current evoked by epilepsy-associated Nanu1.1 mutations. *Br. J Pharmacol.* **161**, 1414-1426 (2010).

62. Kahlig, K. M. *et al.* Ranolazine reduces neuronal excitability by interacting with inactivated states of brain sodium channels. *Mol. Pharmacol.* **85**, 162-174 (2014).

63. Belardinelli, L. *et al.* A novel, potent, and selective inhibitor of cardiac late sodium current suppresses experimental arrhythmias. *J Pharmacol. Exp. Ther.* **344**, 23-32 (2013).

64. Sicouri, S., Belardinelli, L. & Antzelevitch, C. Antiarrhythmic effects of the highly selective late sodium channel current blocker GS-458967. *Heart Rhythm.* **10**, 1036-1043 (2013).

65. Carter, B. C. & Bean, B. P. Sodium entry during action potentials of mammalian neurons: incomplete inactivation and reduced metabolic efficiency in fast-spiking neurons. *Neuron* **64**, 898-909 (2009).

66. Rhodes, T. H., Lossin, C., Vanoye, C. G., Wang, D. W. & George, A. L., Jr. Noninactivating voltage-gated sodium channels in severe myoclonic epilepsy of infancy. *Proc. Natl. Acad. Sci. U. S. A* **101**, 11147-11152 (2004).

67. Kahlig, K. M. *et al.* Divergent sodium channel defects in familial hemiplegic migraine. *Proc. Natl. Acad. Sci. U. S. A.* **105**, 9799-9804 (2008).

68. Thompson, C. H., Kahlig, K. M. & George, A. L., Jr. SCN1A splice variants exhibit divergent sensitivity to commonly used antiepileptic drugs. *Epilepsia* **52**, 1000-1009 (2011).

69. White, H. S. *et al.* The anticonvulsant profile of rufinamide (CGP 33101) in rodent seizure models. *Epilepsia* **49**, 1213-1220 (2008).

70. Frankel, W. N., Taylor, L., Beyer, B., Tempel, B. L. & White, H. S. Electroconvulsive thresholds of inbred mouse strains. *Genomics* **74**, 306-312 (2001).

71. Sloviter, R. S. A simplified Timm stain procedure compatible with formaldehyde fixation and routine paraffin embedding of rat brain. *Brain Res. Bull.* **8**, 771-774 (1982).

72. Kahlig, K. M., Lepist, I., Leung, K., Rajamani, S. & George, A. L. Ranolazine selectively blocks persistent current evoked by epilepsy-associated NaV 1.1 mutations. *Br. J Pharmacol* **161**, 1414-1426 (2010).

73. Dudek, F. E. & Sutula, T. P. Epileptogenesis in the dentate gyrus: a critical perspective. *Prog. Brain Res.* **163**, 755-773 (2007).

74. Buckmaster, P. S. Mossy Fiber Sprouting in the Dentate Gyrus. (2012).

75. Mantegazza, M., Curia, G., Biagini, G., Ragsdale, D. S. & Avoli, M. Voltage-gated sodium channels as therapeutic targets in epilepsy and other neurological disorders. *Lancet Neurol.* **9**, 413-424 (2010).

76. Vanoye, C. G., Lossin, C., Rhodes, T. H. & George, A. L., Jr. Single-channel properties of human $Na_V1.1$ and mechanism of channel dysfunction in SCN1A-associated epilepsy. *J. Gen. Physiol* **127**, 1-14 (2006).

77. Veeramah, K. R. *et al.* De novo pathogenic SCN8A mutation identified by whole-genome sequencing of a family quartet affected by infantile epileptic encephalopathy and SUDEP. *Am. J Hum. Genet.* **90**, 502-510 (2012).

78. Holland, K. D. *et al.* Mutation of sodium channel SCN3A in a patient with cryptogenic pediatric partial epilepsy. *Neurosci Lett.* **433**, 65-70 (2008).

79. Estacion, M., Gasser, A., Dib-Hajj, S. D. & Waxman, S. G. A sodium channel mutation linked to epilepsy increases ramp and persistent current of Nav1.3 and induces hyperexcitability in hippocampal neurons. *Exp. Neurol.* **224**, 362-368 (2010).

80. Chen, S. *et al.* An increase in persistent sodium current contributes to intrinsic neuronal bursting after status epilepticus. *J Neurophysiol.* **105**, 117-129 (2011).

81. Lin, W. H., Gunay, C., Marley, R., Prinz, A. A. & Baines, R. A. Activity-dependent alternative splicing increases persistent sodium current and promotes seizure. *J Neurosci.* **32**, 7267-7277 (2012).

82. Sun, L. *et al.* A knock-in model of human epilepsy in Drosophila reveals a novel cellular mechanism associated with heat-induced seizure. *J Neurosci.* **32**, 14145-14155 (2012).

83. Nissinen, J., Large, C. H., Stratton, S. C. & Pitkanen, A. Effect of lamotrigine treatment on epileptogenesis: an experimental study in rat. *Epilepsy Res.* **58**, 119-132 (2004).

84. Pitkanen, A., Nissinen, J., Jolkkonen, E., Tuunanen, J. & Halonen, T. Effects of vigabatrin treatment on status epilepticus-induced neuronal damage and mossy fiber sprouting in the rat hippocampus. *Epilepsy Res.* **33**, 67-85 (1999).

85. Cha, B. H., Akman, C., Silveira, D. C., Liu, X. & Holmes, G. L. Spontaneous recurrent seizure following status epilepticus enhances dentate gyrus neurogenesis. *Brain Dev.* **26**, 394-397 (2004).

86. Buckmaster, P. S. Prolonged infusion of tetrodotoxin does not block mossy fiber sprouting in pilocarpine-treated rats. *Epilepsia* **45**, 452-458 (2004).

87. Buckmaster, P. S., Ingram, E. A. & Wen, X. Inhibition of the mammalian target of rapamycin signaling pathway suppresses dentate granule cell axon sprouting in a rodent model of temporal lobe epilepsy. *J Neurosci.* **29**, 8259-8269 (2009).

88. Kwan, P., Schachter, S. C. & Brodie, M. J. Drug-resistant epilepsy. *N. Engl. J. Med.* **365**, 919-926 (2011).

89. Rhodes, T. H. *et al.* Sodium channel dysfunction in intractable childhood epilepsy with generalized tonic-clonic seizures. *J. Physiol* **569**, 433-445 (2005).